フラクタル構造を有する超伝導複合化合物の位相コヒーレンス形成

神戸大学大学院理学研究科　化学専攻

内 野　隆 司

共同研究者:
神戸大学：櫻井敬博先生，太田仁先生，瀬戸雄介先生（大阪公立大）
NIMS: 大井修一博士，有沢俊一博士，立木実博士

超伝導体/常伝導体(絶縁体)界面における超伝導近接効果

superconductor insulator superconductor

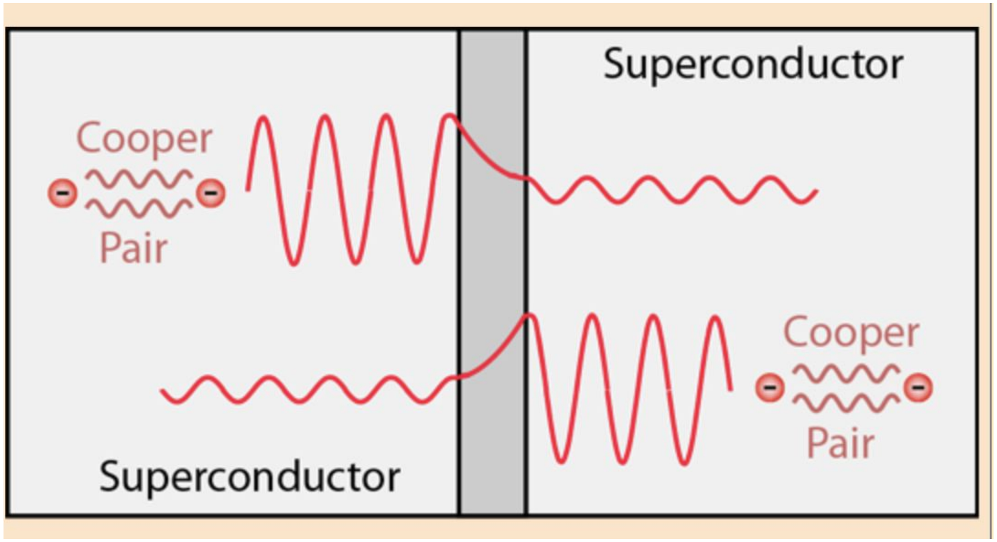

S I S

S/I/S Josephson junction: tunneling of Cooper pairs

$$I(t) = I_c \sin(\varphi(t))$$

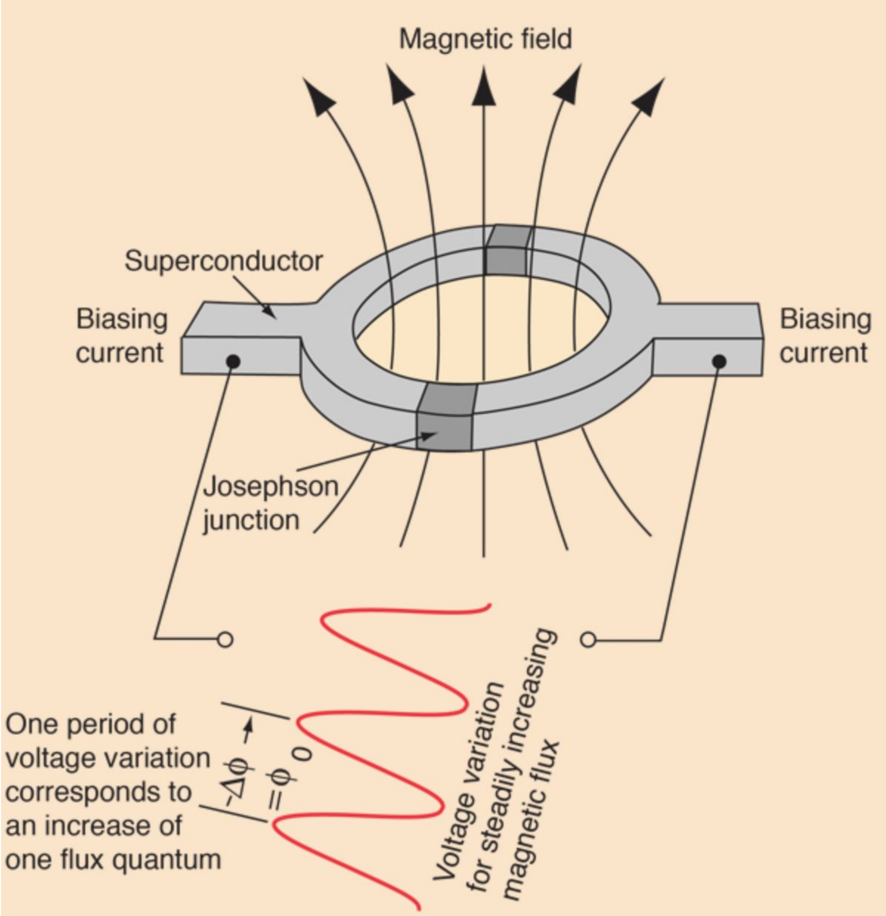

Superconducting quantum interference device (SQUID)

超伝導体/常伝導体(金属)界面における超伝導近接効果

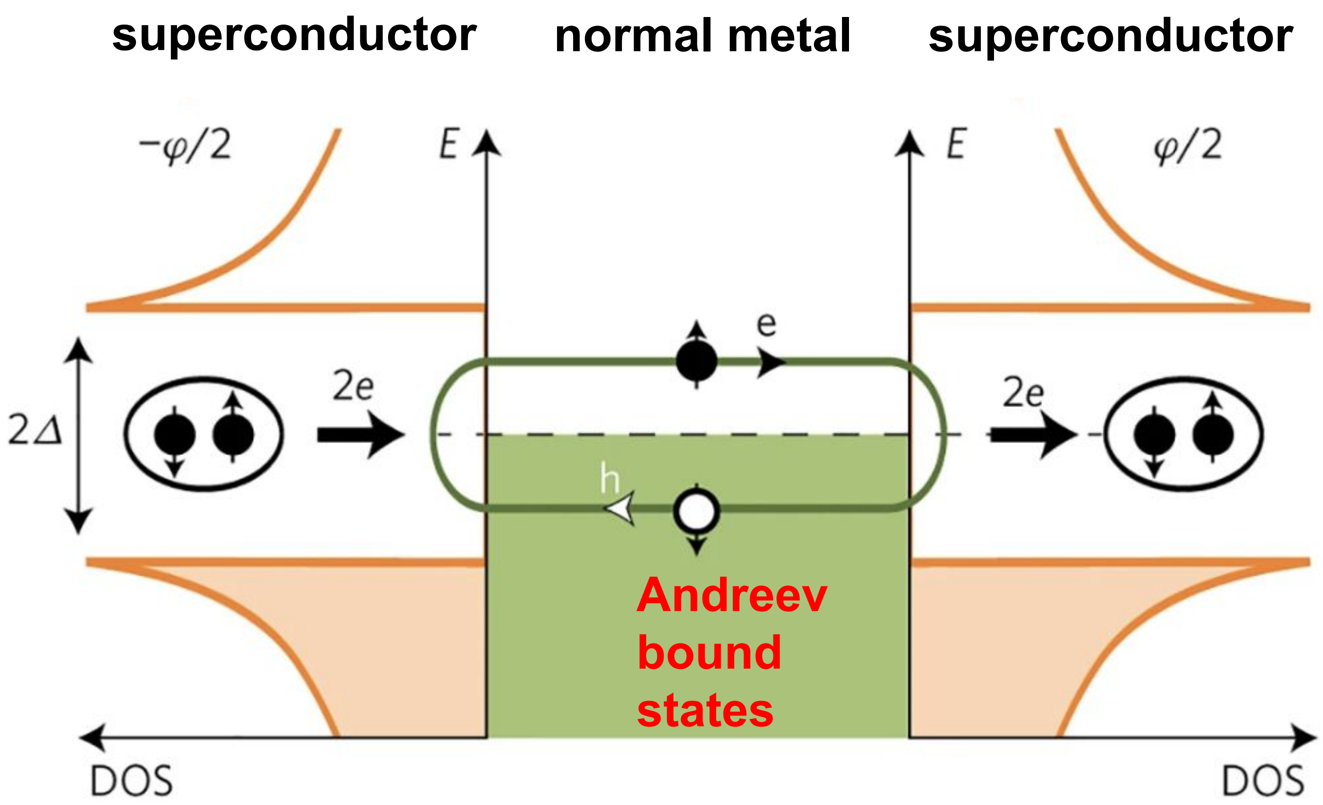

L. Bretheau et al.
Nat. Phys. **13**, 756 (2017).

S/N/S Josephson junction: Andreev reflection(アンドレーエフ反射)

超伝導体/常伝導体（金属）界面における超伝導近接効果

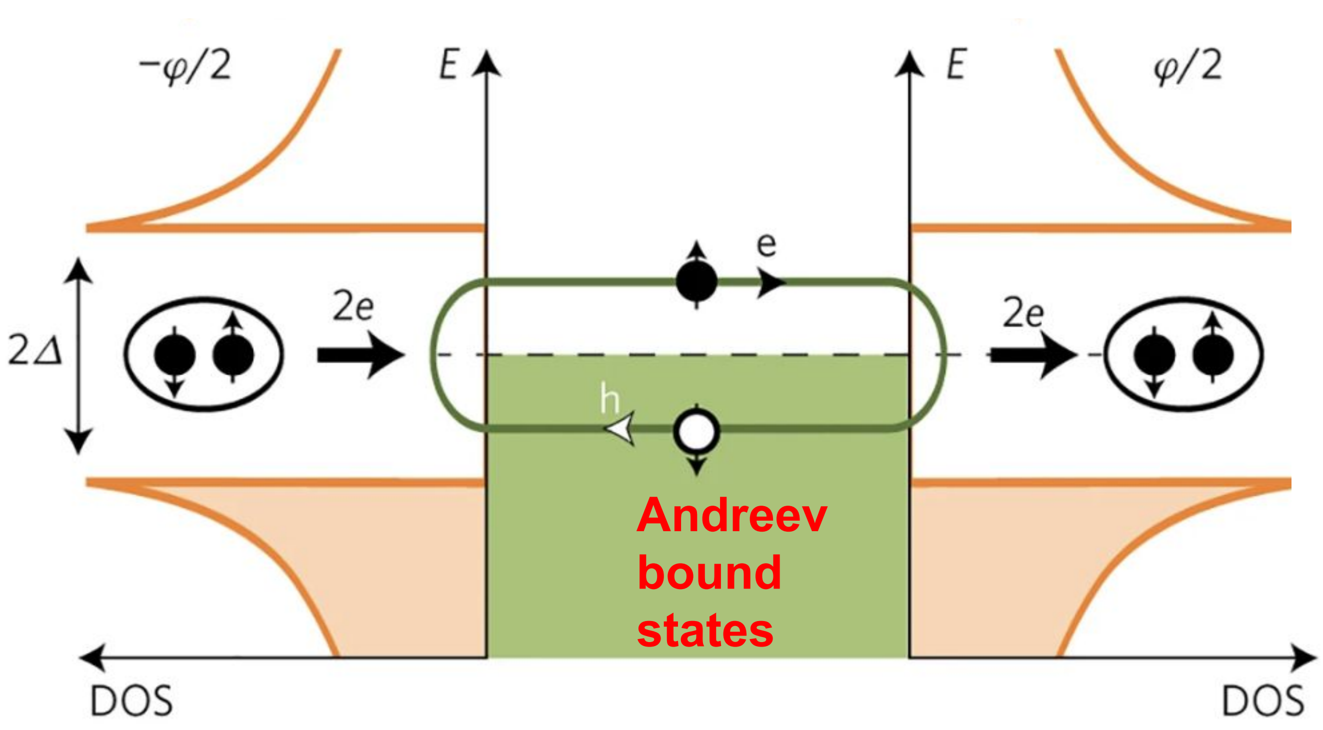

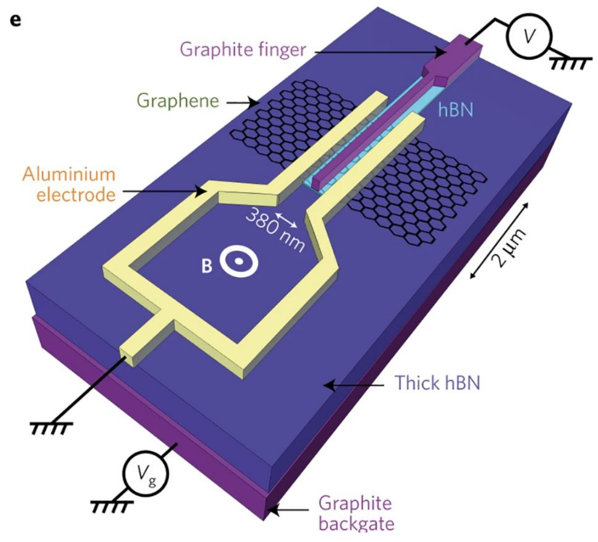

L. Bretheau et al.
Nat. Phys. **13**, 756 (2017).

S/N/S Josephson junction: Andreev reflection（アンドレーエフ反射）

超伝導体/常伝導体（金属）界面における超伝導近接効果

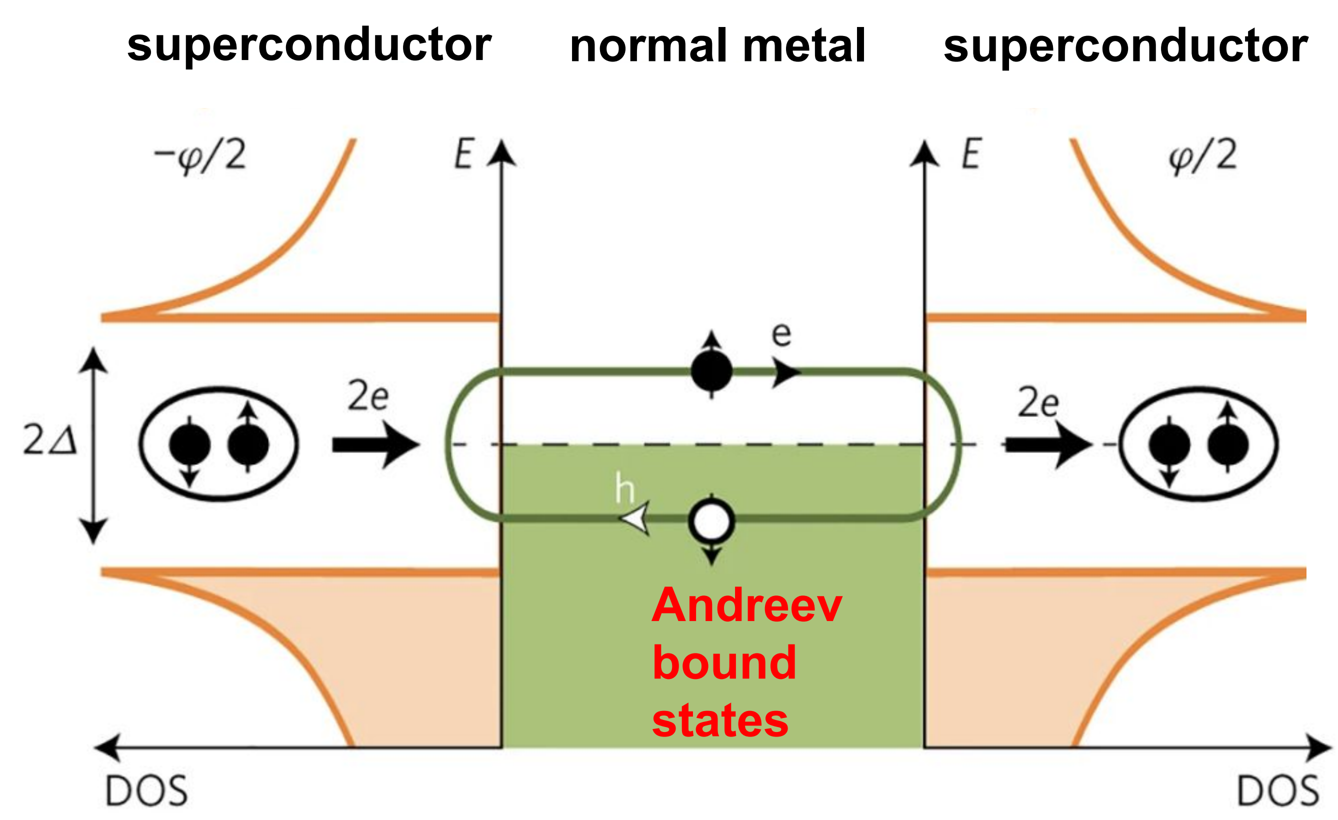

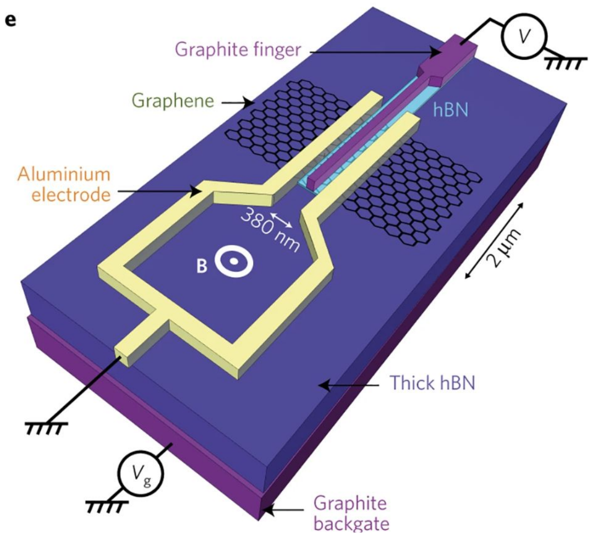

L. Bretheau et al.
Nat. Phys. **13**, 756 (2017).

S/N/S Josephson junction: Andreev reflection（アンドレーエフ反射）

本研究：フラクタル分布した超伝導SNS複合体の超伝導近接効果による位相コヒーレンス形成

自然界におけるフラクタル構造

フラクタル：図形の全体をいくつかの部分に分解していった時に
全体と同じ形が再現されていく構造（自己相似構造）

オウム貝

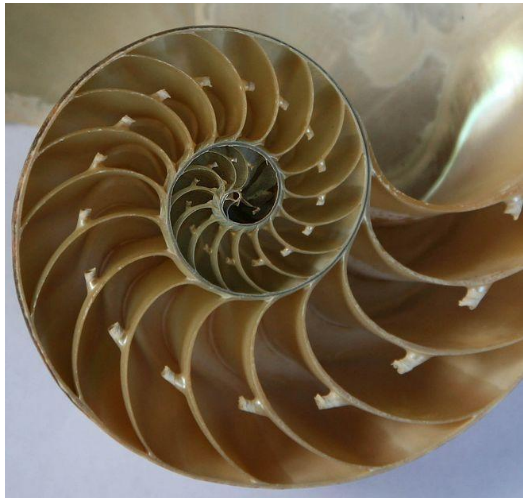

ロマネスコ（ブロッコリー）

樹枝

氷の結晶成長

ニューラルネットワーク

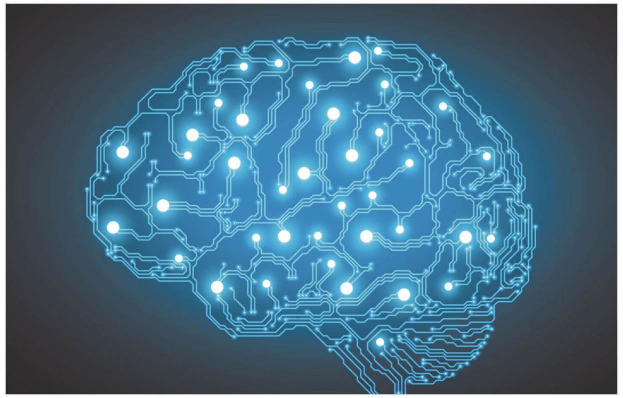

World Wide Web (WWW)

https://ewm.swiss/en/blog/history-world-wide-web

フラクタルネットワークの特徴

nature physics | VOL 2 | APRIL 2006 | 275

ARTICLES

Origins of fractality in the growth of complex networks

CHAOMING SONG[1], SHLOMO HAVLIN[2] AND HERNÁN A. MAKSE[1]*

[1]Levich Institute and Physics Department, City College of New York, New York, New York 10031, USA
[2]Minerva Center and Department of Physics, Bar-Ilan University, Ramat Gan 52900, Israel
*e-mail: makse@mailaps.org

Complex networks from such different fields as biology, technology or sociology share similar organization principles. The possibility of a unique growth mechanism promises to uncover universal origins of collective behaviour. In particular, the emergence of self-similarity in complex networks raises the fundamental question of the growth process according to which these structures evolve. Here we investigate the concept of renormalization as a mechanism for the growth of fractal and non-fractal modular networks. We show that the key principle that gives rise to the fractal architecture of networks is a strong effective 'repulsion' (or, disassortativity) between the most connected nodes (that is, the hubs) on all length scales, rendering them very dispersed. More importantly, we show that a robust network comprising functional modules, such as a cellular network, necessitates a fractal topology, suggestive of an evolutionary drive for their existence.

自己相似性

階層性

↓

Positive feedback
Collective synchronization
Self organization
Network robustness, etc

PRL 96, 018701 (2006) PHYSICAL REVIEW LETTERS week ending 13 JANUARY 2006

Skeleton and Fractal Scaling in Complex Networks

K.-I. Goh, G. Salvi, B. Kahng, and D. Kim
School of Physics and Center for Theoretical Physics, Seoul National University, Seoul 151-747, Korea
(Received 13 August 2005; published 11 January 2006)

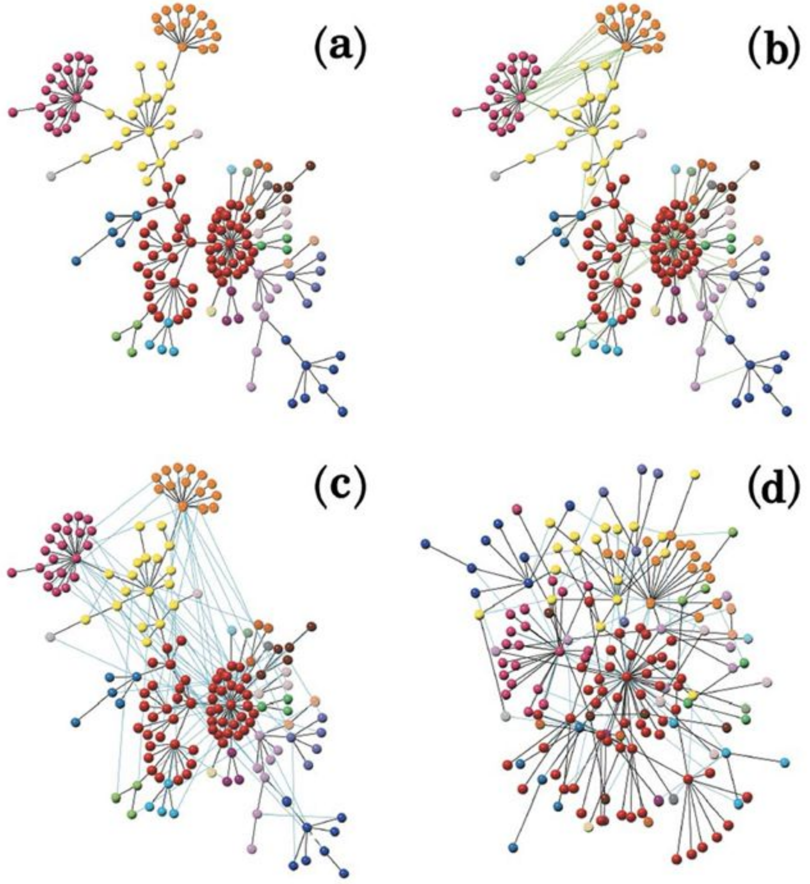

Scale-free structural organization of oxygen interstitials in La_2CuO_{4+y}

M. Fratini *et al*. Nature, 466, 841 (2010).

Michela Fratini[1]†, Nicola Poccia[1], Alessandro Ricci[1], Gaetano Campi[1,2], Manfred Burghammer[3], Gabriel Aeppli[4] & Antonio Bianconi[1]

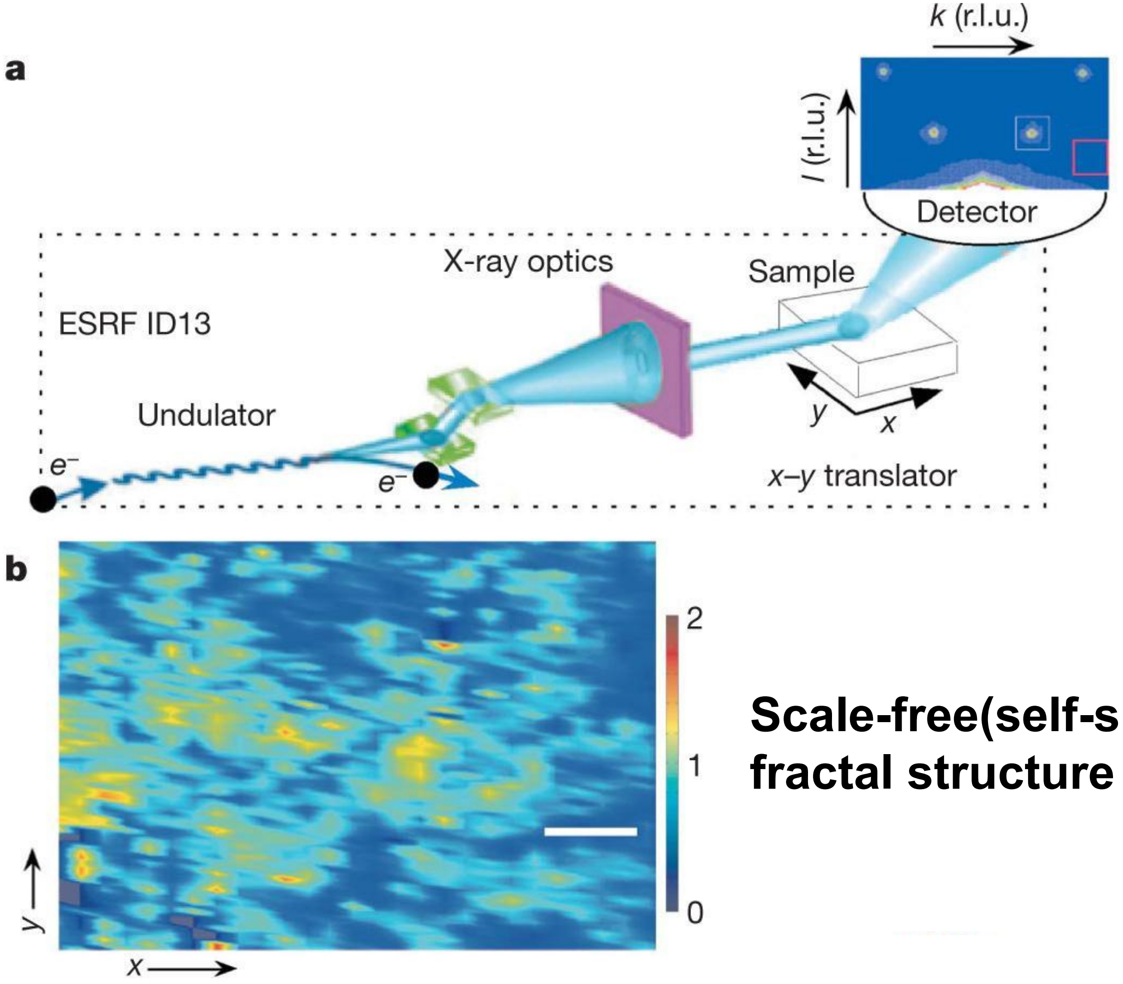

Figure 1 | Mixed real- and reciprocal-space images of dopant ordering. a, The X-ray microdiffraction apparatus is located at the European Synchrotron Radiation Facility (ESRF)

The intense red–yellow peaks represent locations in the sample with high strength of the three-dimensional interstitial oxygen (i-O) ordering, and dark blue indicates spots of disordered i-O domains.

Scale-free(self-similar) fractal structure

Fractal structures enhance the superconductivity

M. Fratini *et al*. Nature, 466, 841 (2010).

Distribution of oxygen interstitials

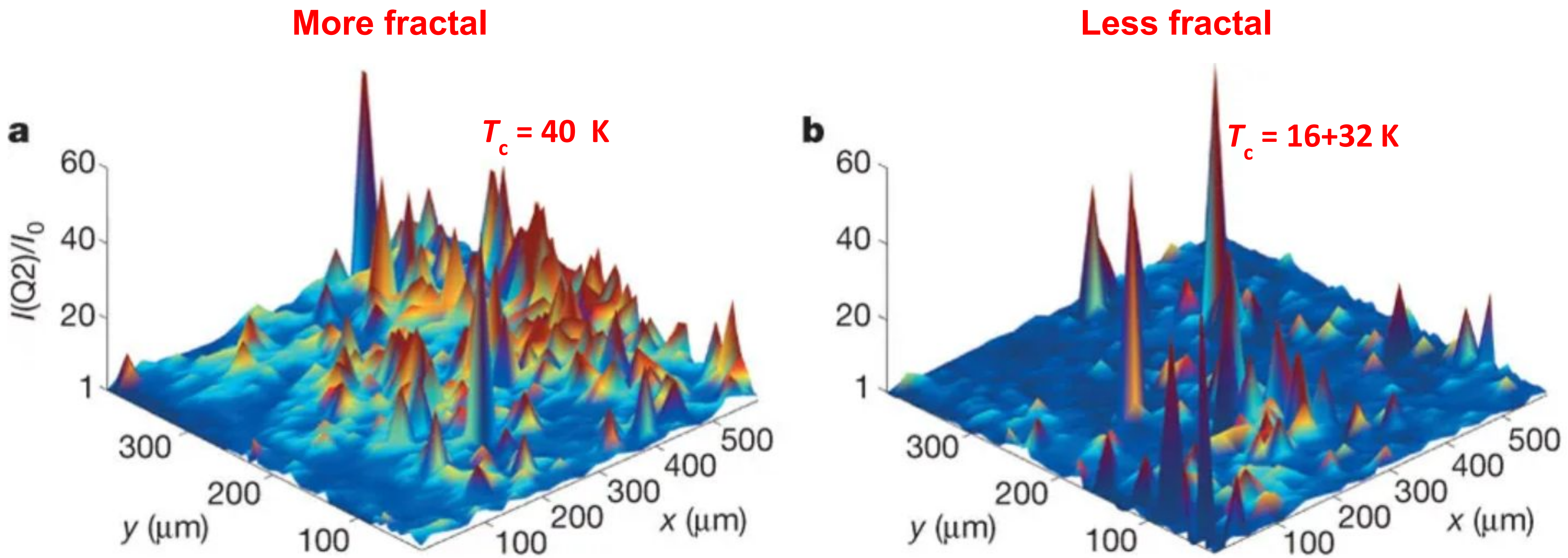

ユニットセルの周期配列に基づくバンド理論
とは異なる電子構造の発現の可能性

Question:

超伝導体微粒子が常伝導マトリックス中にフラクタル的に分散したらどうなるだろうか?

⇩

$Mg/MgO/MgB_2$ ナノ複合体

Mg/MgO/MgB_2 ナノ複合体の合成

$$B_2O_3 + 5\ Mg \longrightarrow 3\ MgO + Mg + MgB_2$$

700 °C, 3h, under flowing Ar atmosphere

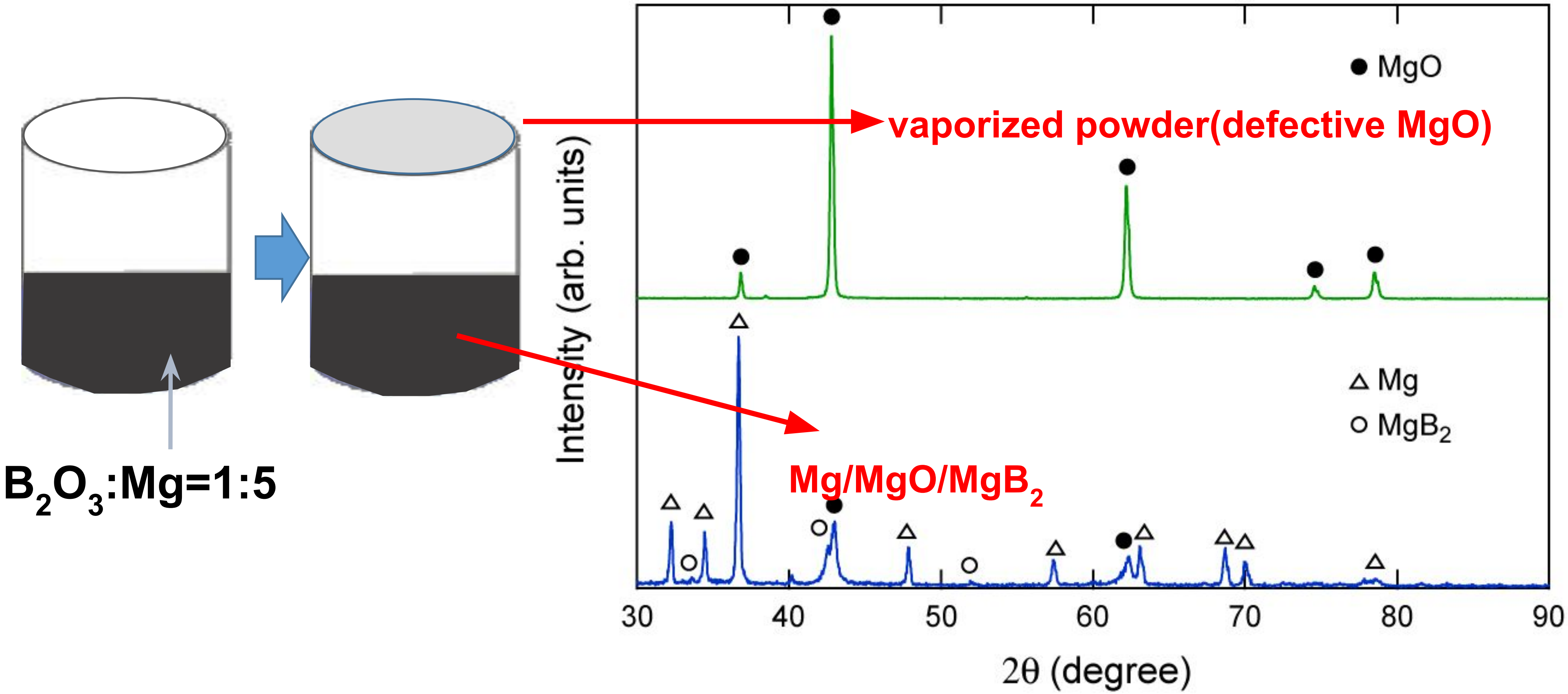

発光強度の励起フルエンス依存性

Excitation: A pulsed Nd:YAG laser (λ=266 nm, pulse width 8ns, repetition rate 10 Hz)
Beam spot size: φ=3mm

Y. Uenaka and T. Uchino *et al.*
PRL **101**, 117401 (2008).
PRB **79**, 165107 (2009).
PRB **83**, 195108 (2011).

SEM Image

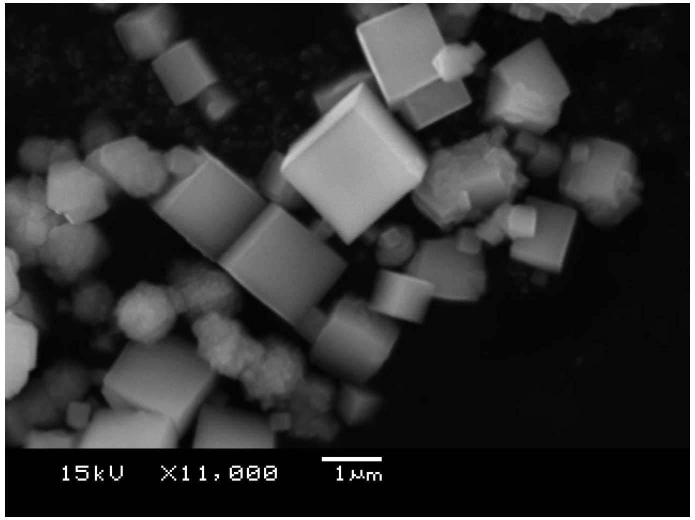

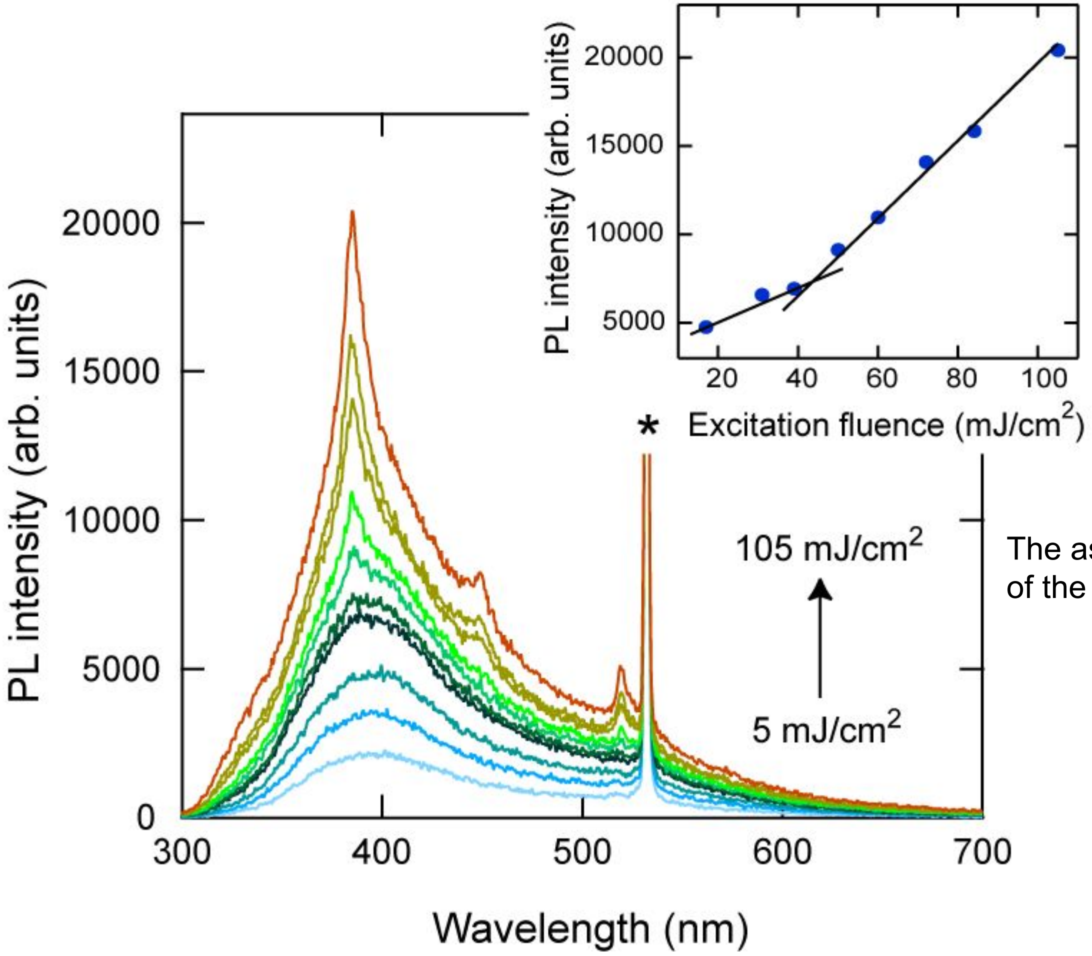

The asterisk (*) indicates the second harmonic (532 nm) of the Nd:YAG laser contaminated in the incident beam.

MgO中の酸素空孔（カラーセンター）による室温ランダムレーザー発振

$Mg/MgO/MgB_2$ ナノ複合体の合成

$$B_2O_3 + 5\ Mg \longrightarrow 3\ MgO + Mg + MgB_2$$

700 °C, 3h, under flowing Ar atmosphere

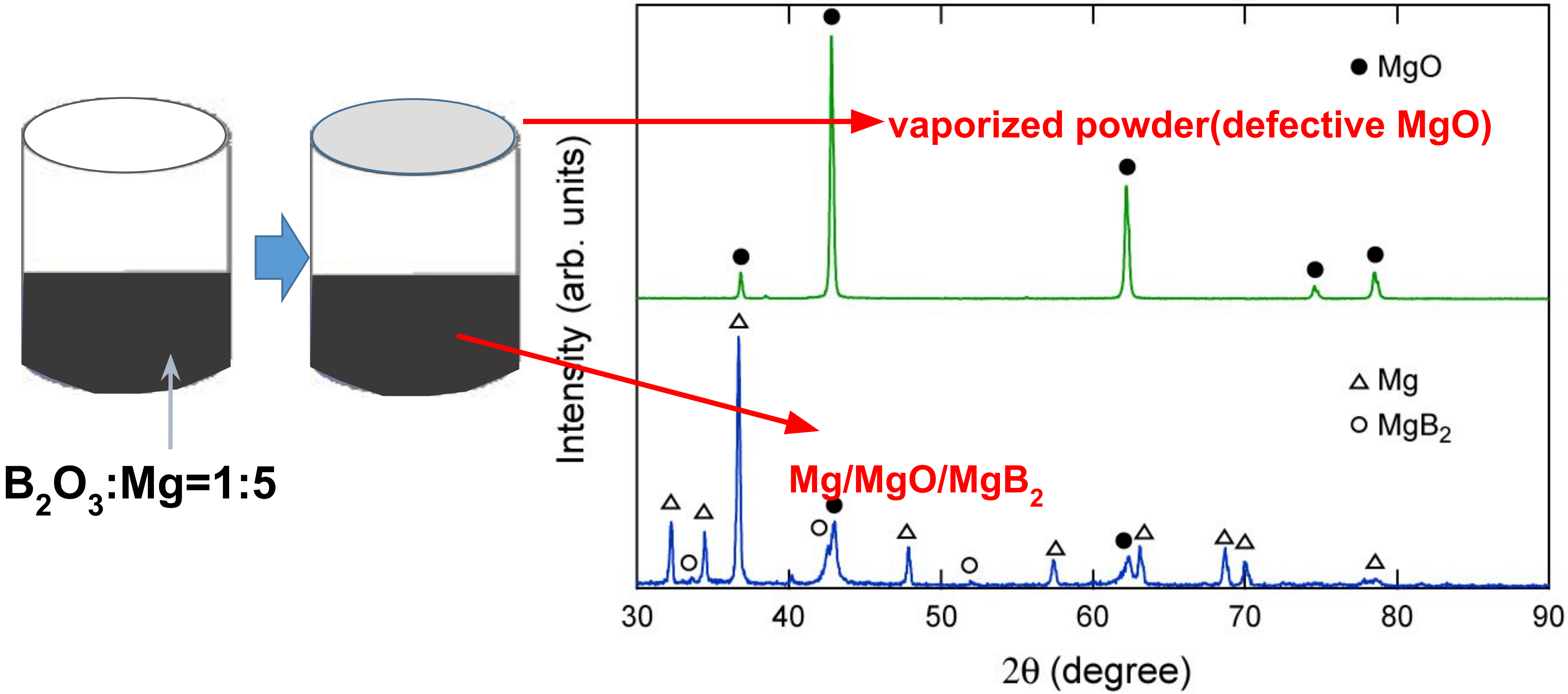

RAPID COMMUNICATIONS

PHYSICAL REVIEW B **74**, 161306(R) (2006)

Ferromagnetism as a universal feature of nanoparticles of the otherwise nonmagnetic oxides

A. Sundaresan,* R. Bhargavi, N. Rangarajan, U. Siddesh, and C. N. R. Rao
Chemistry and Physics of Materials Unit and Department of Science and Technology Unit on Nanoscience, Jawaharlal Nehru Centre for Advanced Scientific Research, Jakkur P. O., Bangalore 560 064 India
(Received 18 August 2006; published 20 October 2006)

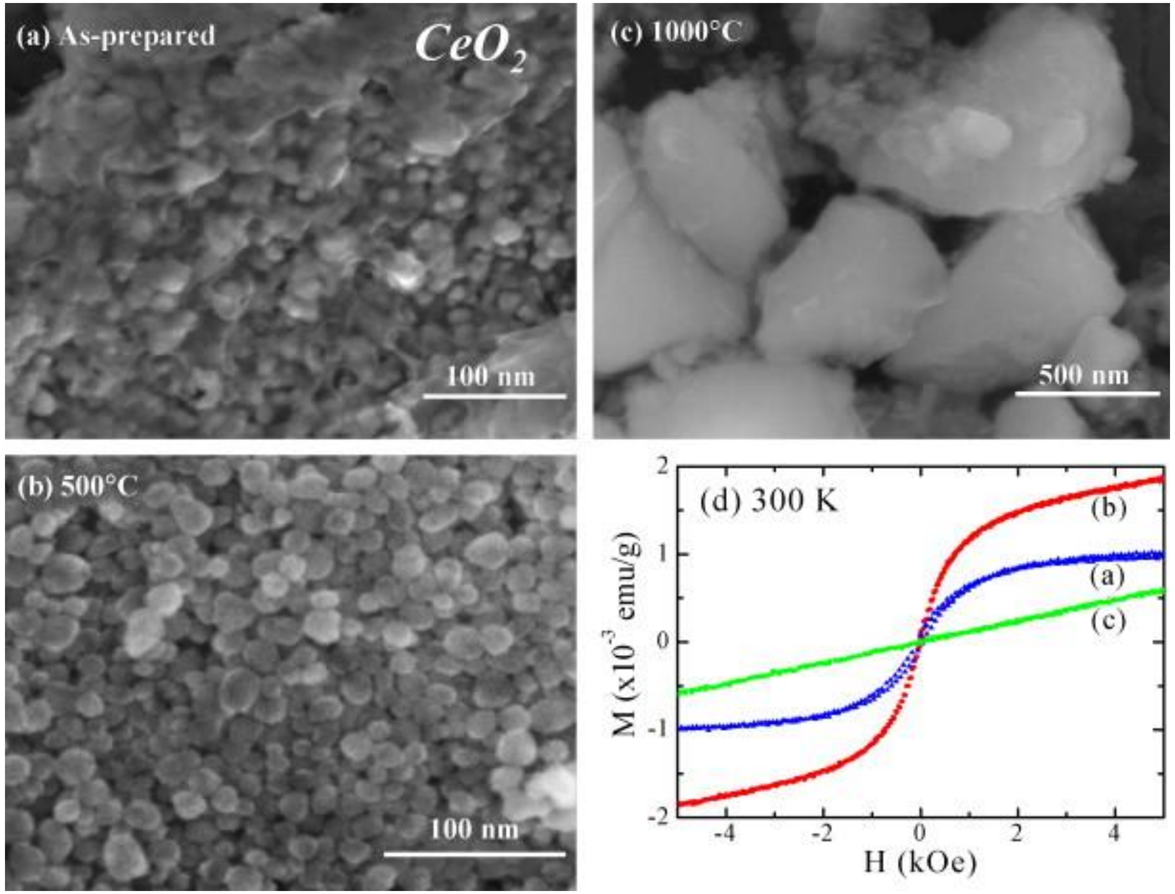

Spin Density Distribution of cation vacancies at (100) MgO surface

(1 0 0)

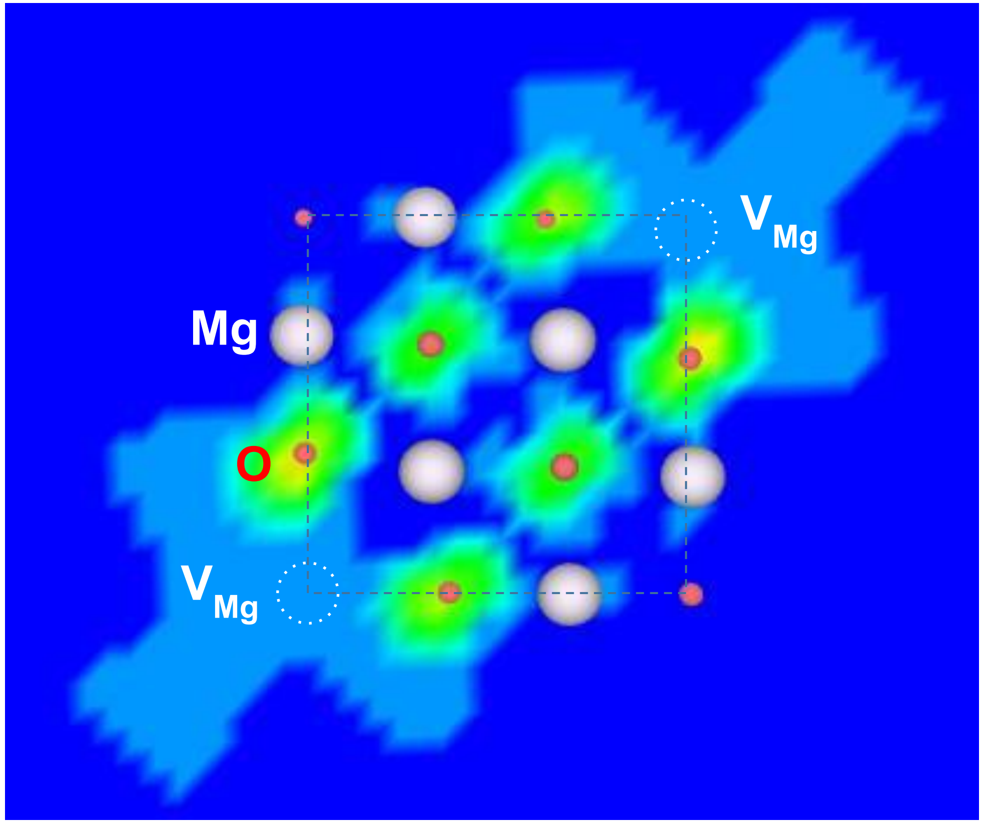

T. Uchino and T. Yoko,
Phys. Rev. B **85**, 012407 (2012);
Phys. Rev. B **87**, 144414 (2013).

Directional spin delocalization over the low-coordinated surface O atoms

Ferromagnetic nanostructures

Magnetic properties of the Mg/MgO/MgB_2 nanocomposite

T. Uchino, Y. Uenaka, H. Soma, T. Sakurai, and H. Ohta, *J. Appl. Phys*. **115**, 063910 (2014).

M(*H*)

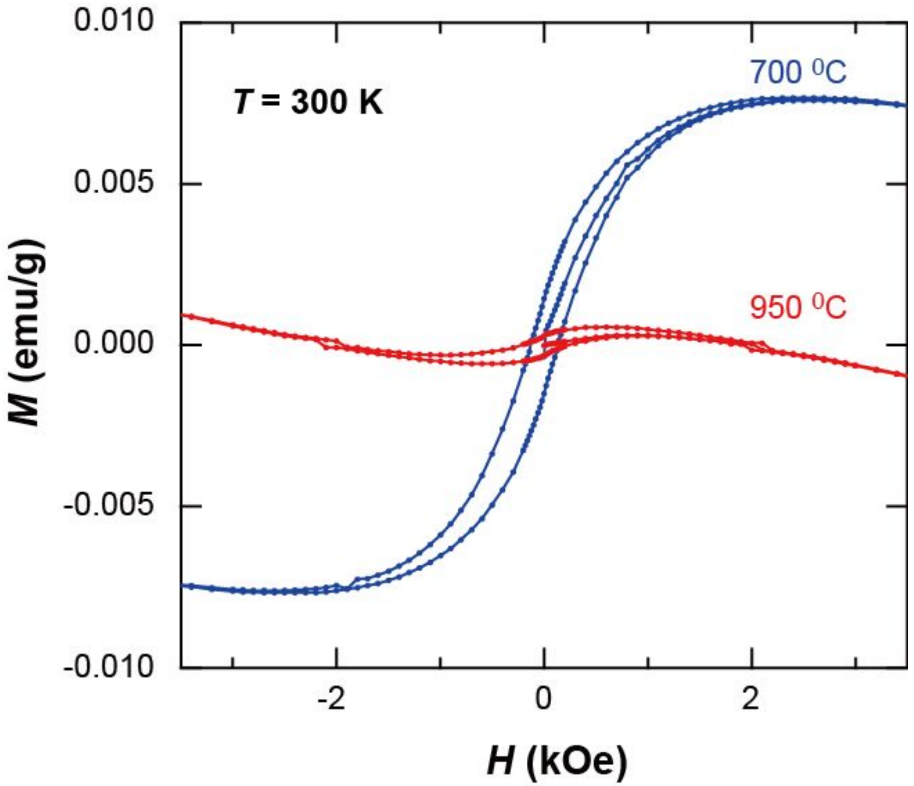

室温で強磁性的ヒステリシス

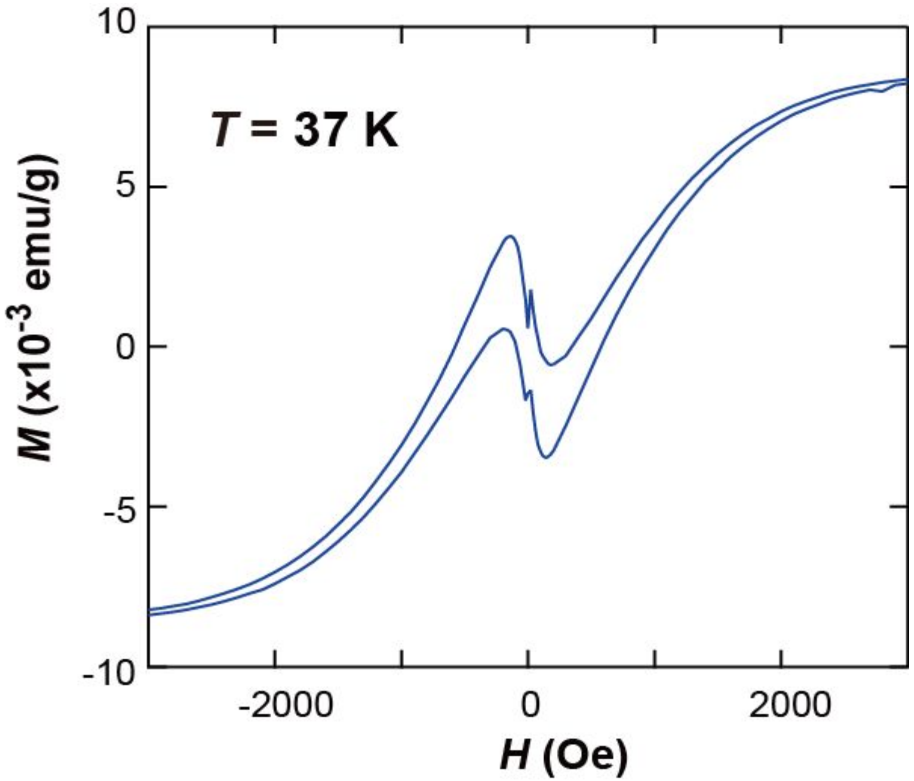

低温で強磁性と超伝導的なヒステリシスが共存

Magnetic properties of the Mg/MgO/MgB_2 nanocomposite

T. Uchino, Y. Uenaka, H. Soma, T. Sakurai, and H. Ohta, *J. Appl. Phys*. **115**, 063910 (2014).

***M*(*H*)**

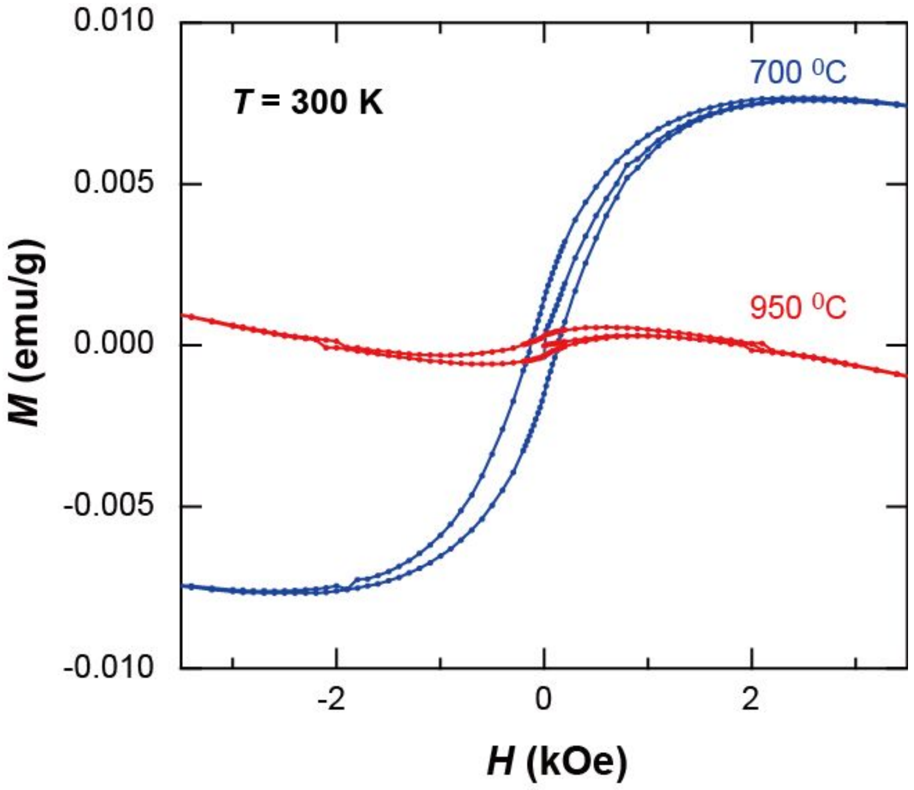

室温で強磁性的ヒステリシス

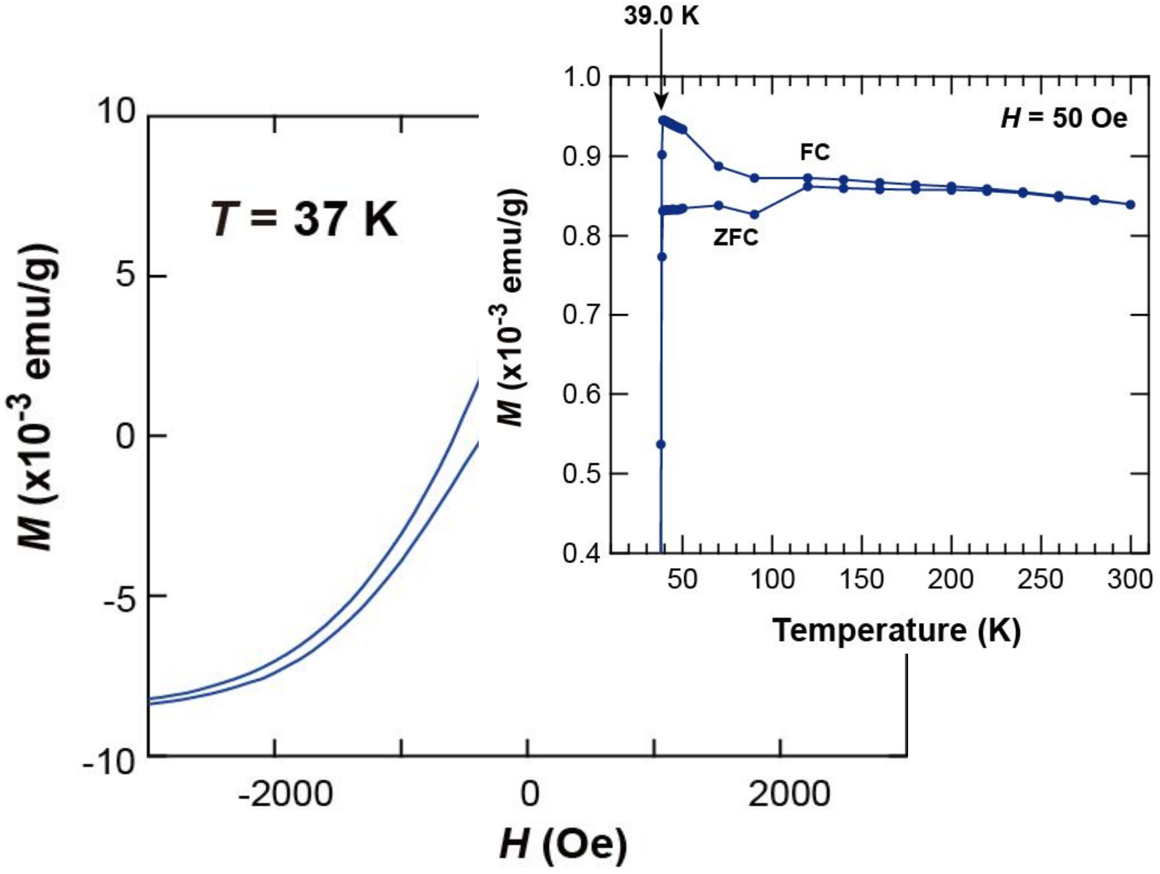

低温で強磁性と超伝導的なヒステリシスが共存

Spark Plasma Sintering (SPS)

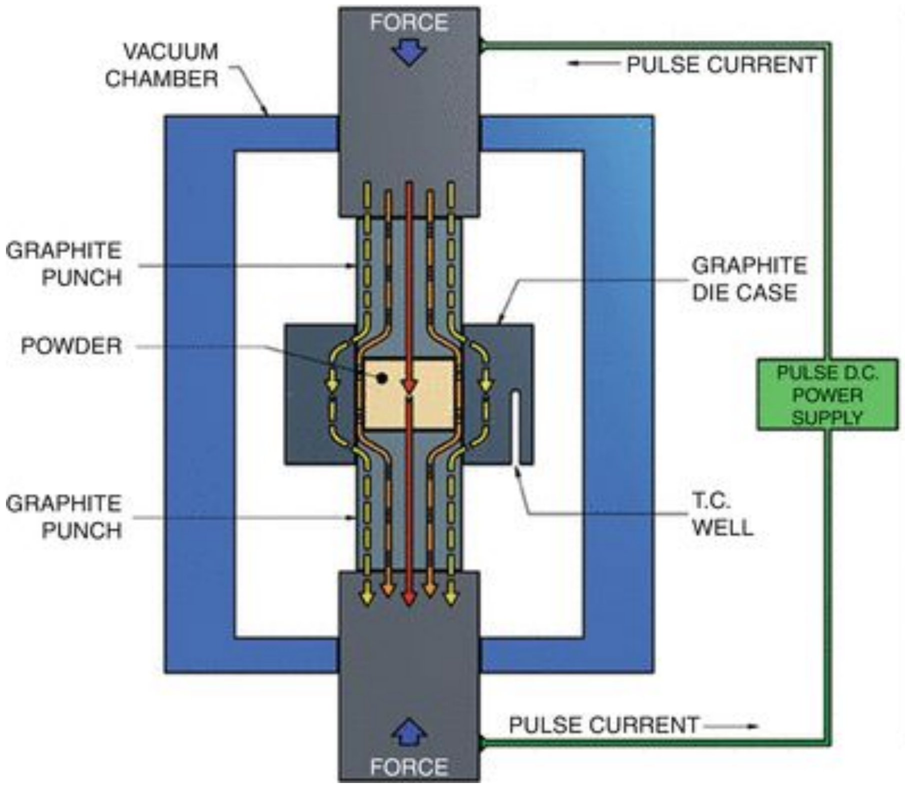

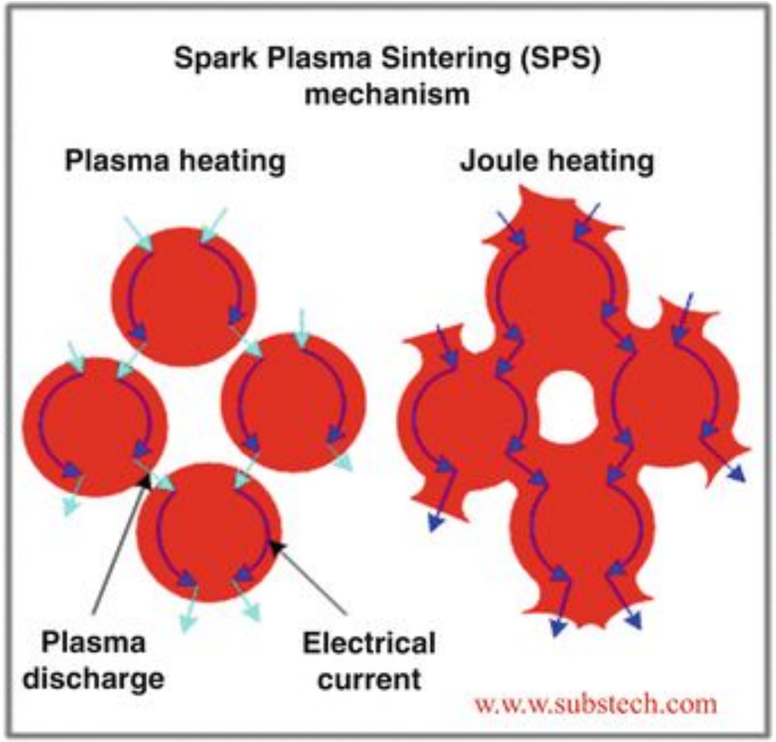

Nano-sized powders can be sintered without considerable grain growth.

No coarsening and no grain growth: high relative densities in very short time

XRD pattern of the SPS-treated sample:

Sintering temperature: 650 °C
Uniaxial pressure: 100 Mpa
Dynamic vacuum: ~50 Pa

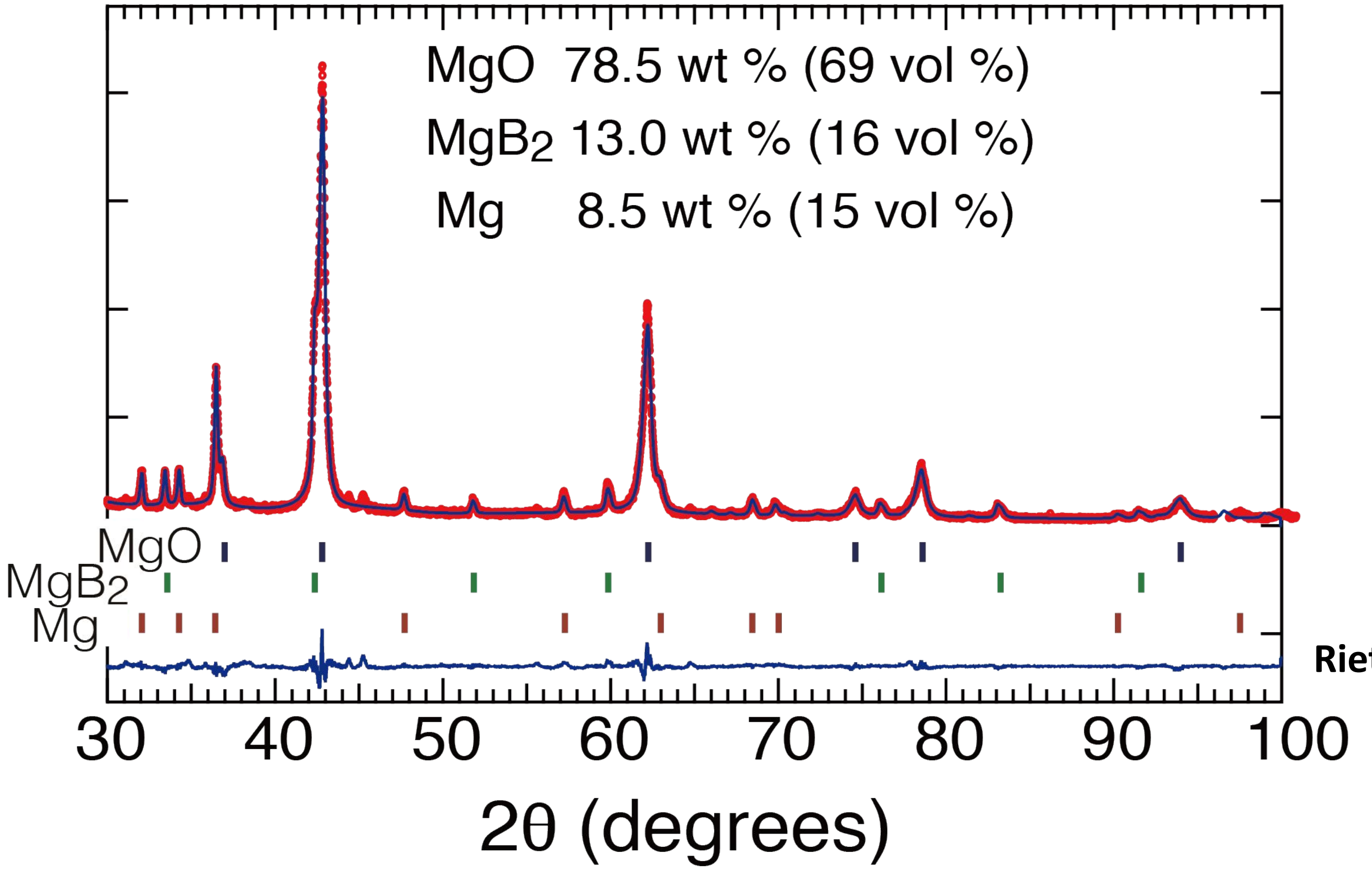

Rietveld fitting

Volume fraction of MgB_2 is well below the percolation threshold (~30 %).

FESEM/EDX, TEM/EDX and HR-TEM measurements

T. Uchino, N. Teramachi *et al.*, *Phys. Rev. B* **101**, 035146 (2020).

B: red
Mg: blue
O: green

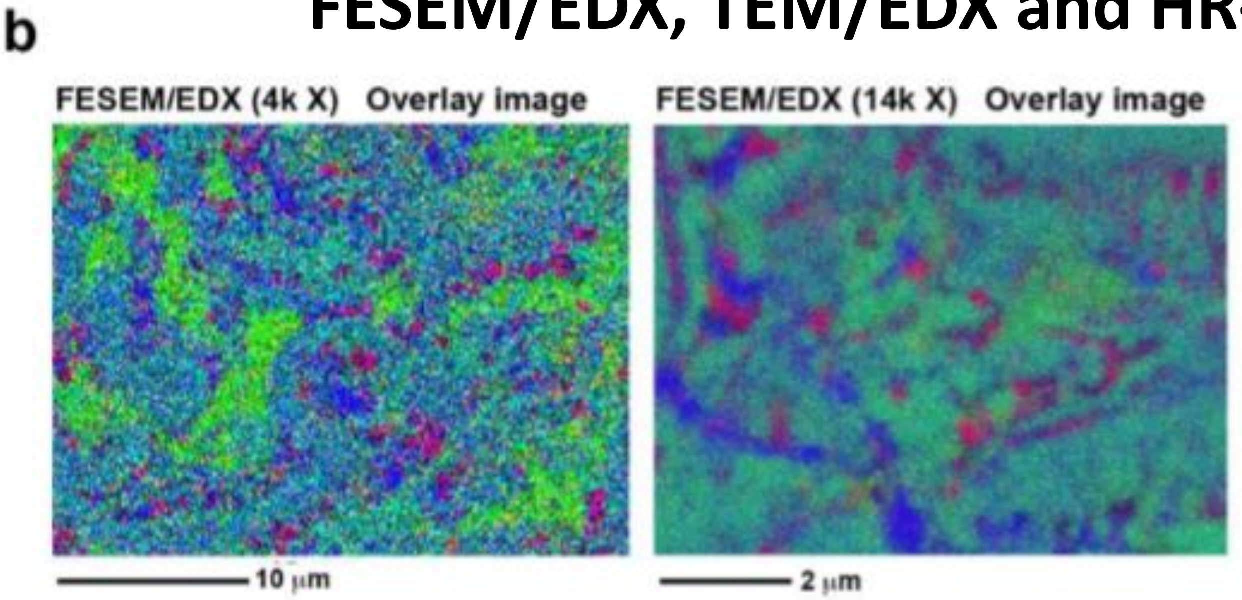

Low (x4,000) Magnification **Medium (x14,000) Magnification**

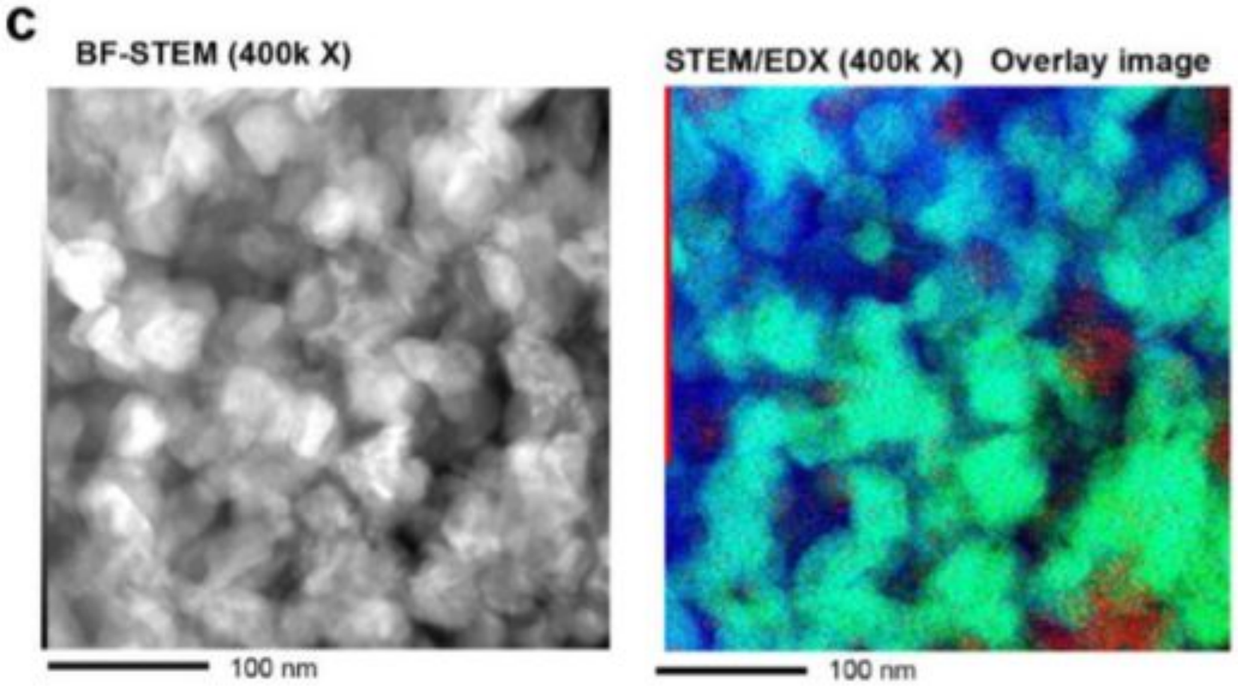

High (x4,000,000) Magnification

HR-TEM

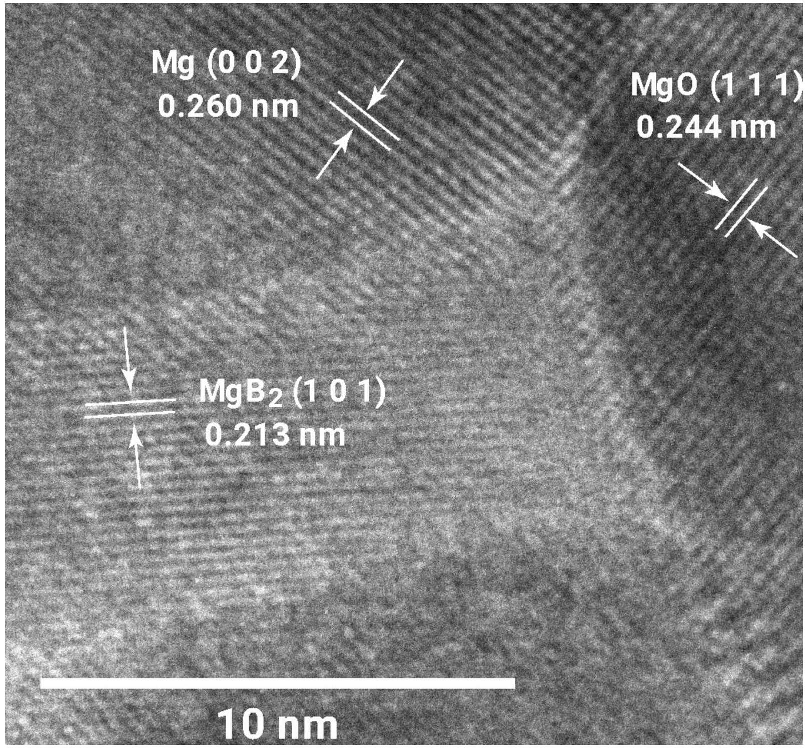

Clean interfaces

Estimation of fractal dimension by the box counting method

An object is covered by a grid of boxes of side length *r* and the number of boxes *N* intercepted by the object is counted.

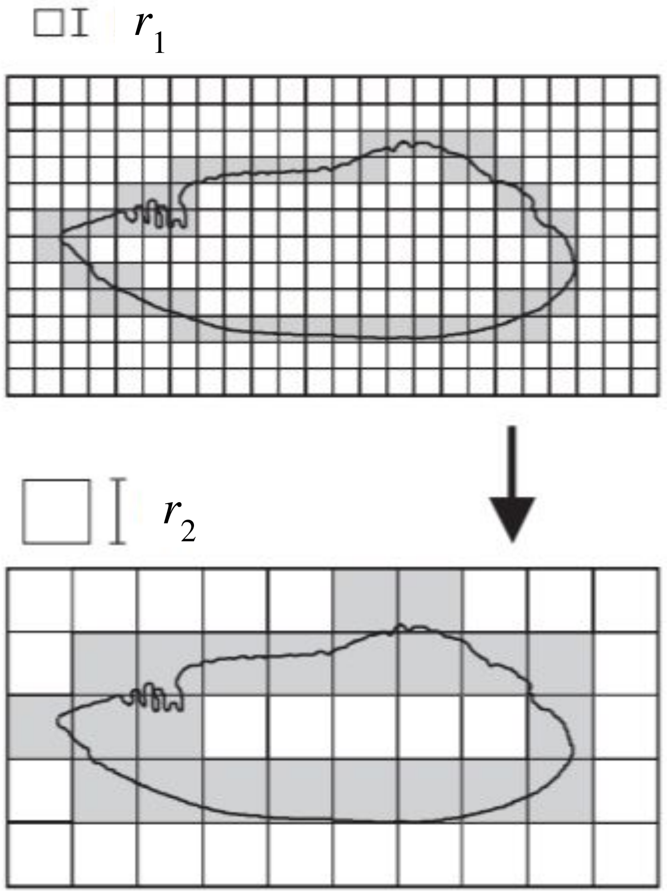

Fractal dimension

$$D = -\frac{\log N}{\log r}$$

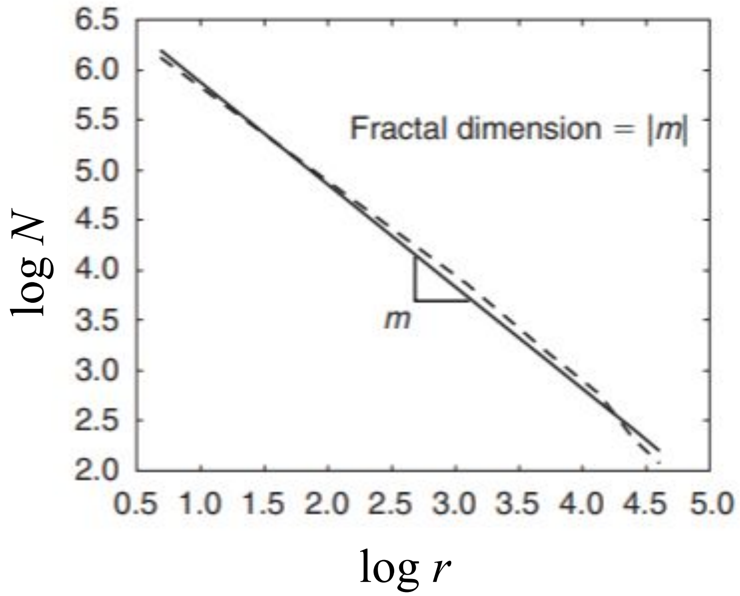

FESEM/EDX, TEM/EDX and HR-TEM measurements

B: red
Mg: blue
O: green

b

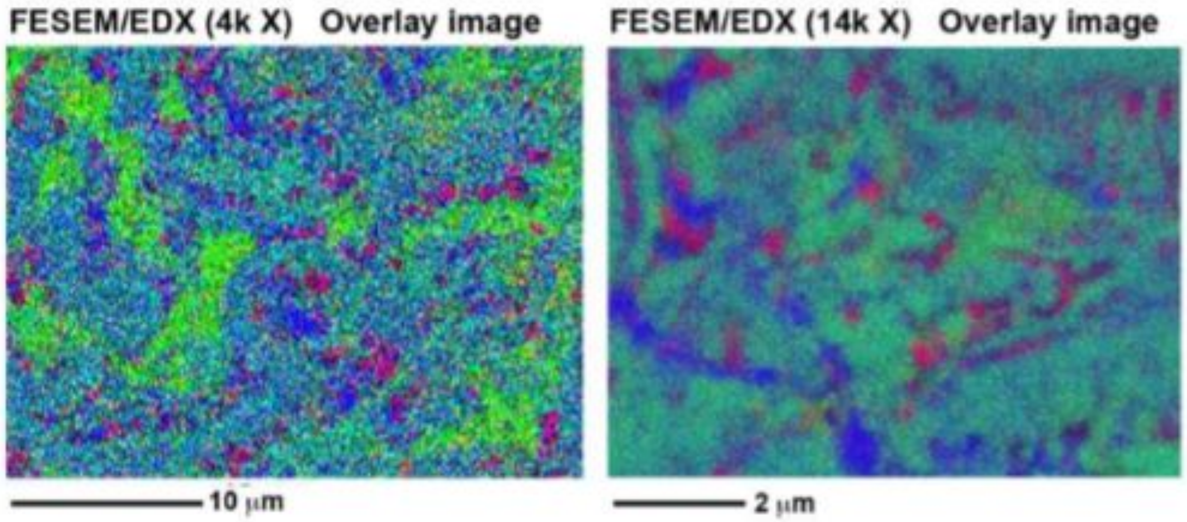

Low (x4,000) Magnification

Medium (x14,000) Magnification

c

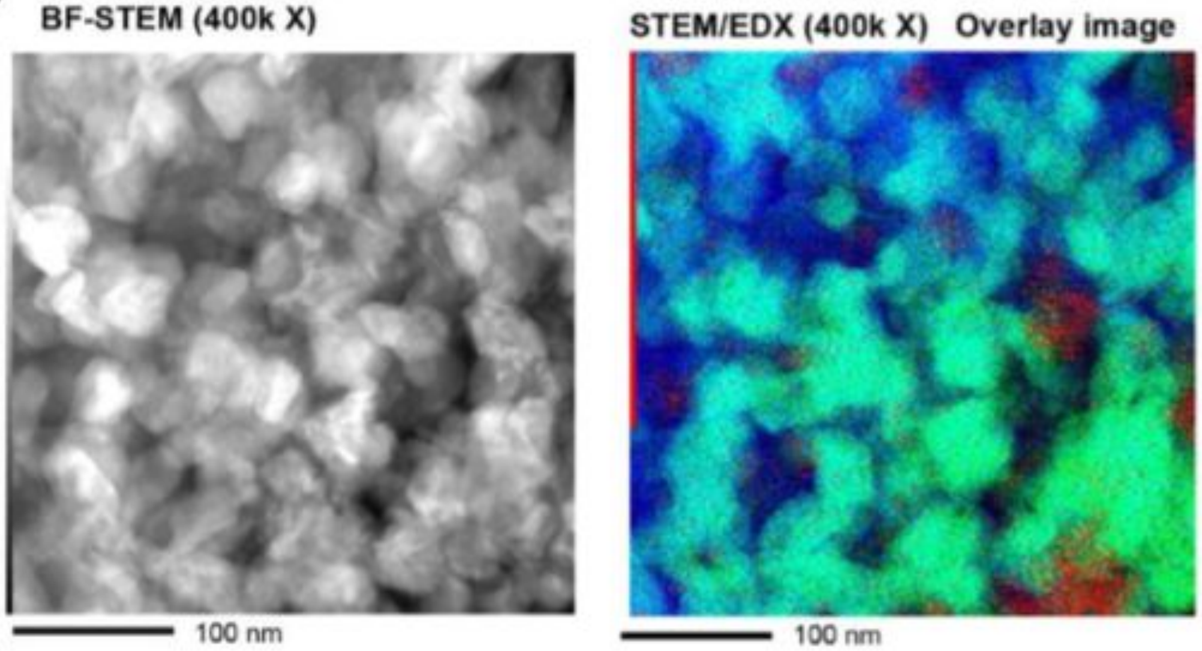

HR-TEM

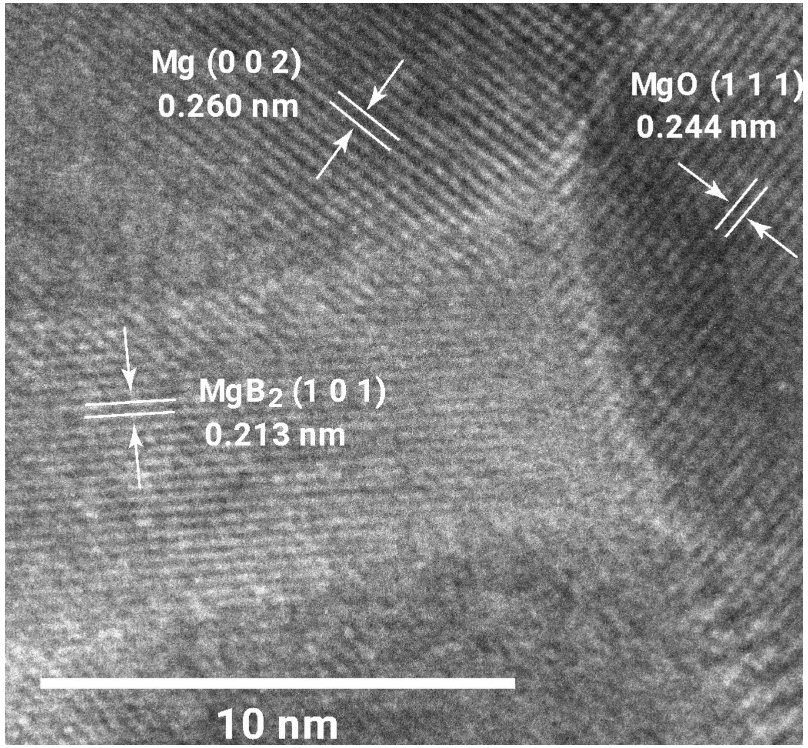

Clean interfaces

High (x4,000,000) Magnification

Fractal analysis of boron distribution: box counting method

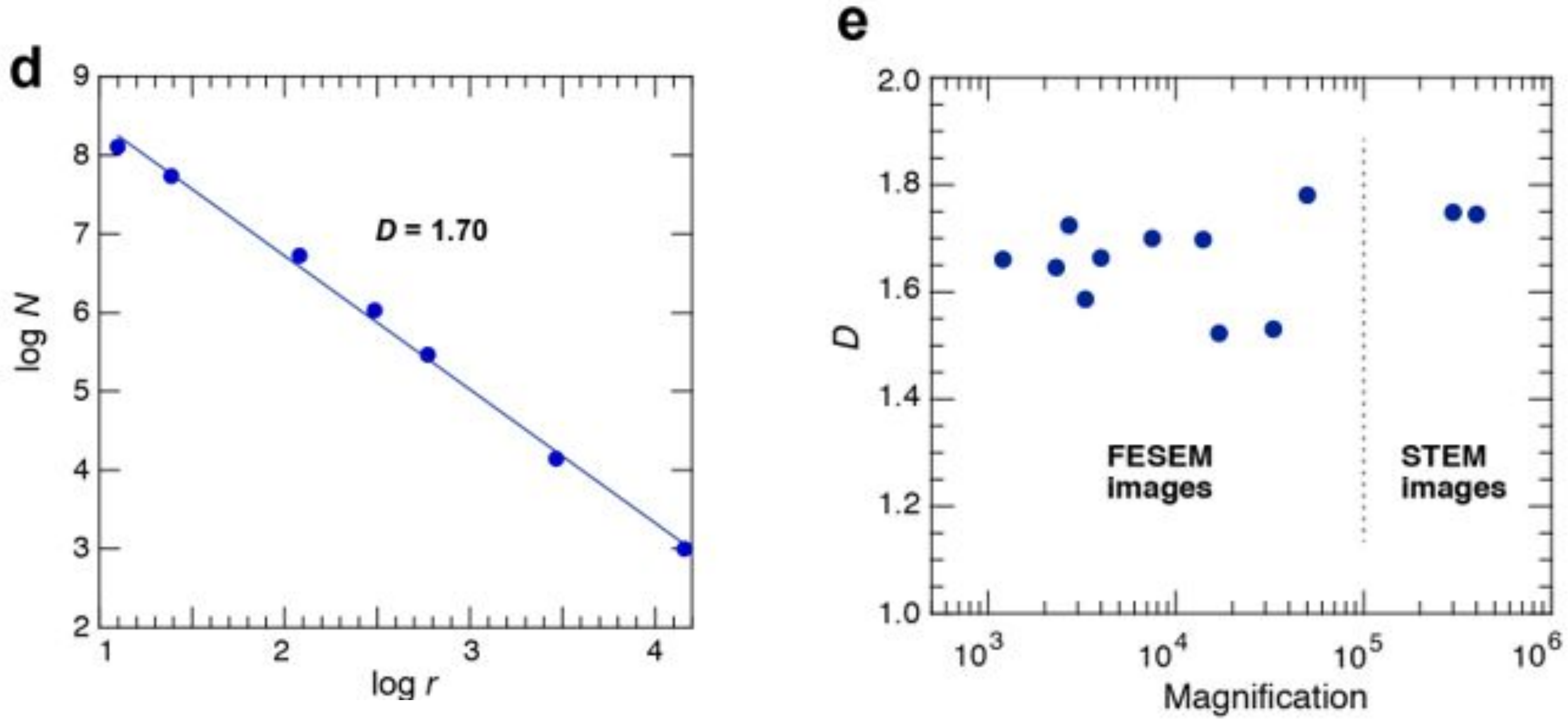

Superconducting properties

Electrical resistivity ρ and magnetic susceptibility χ measurements

R-T

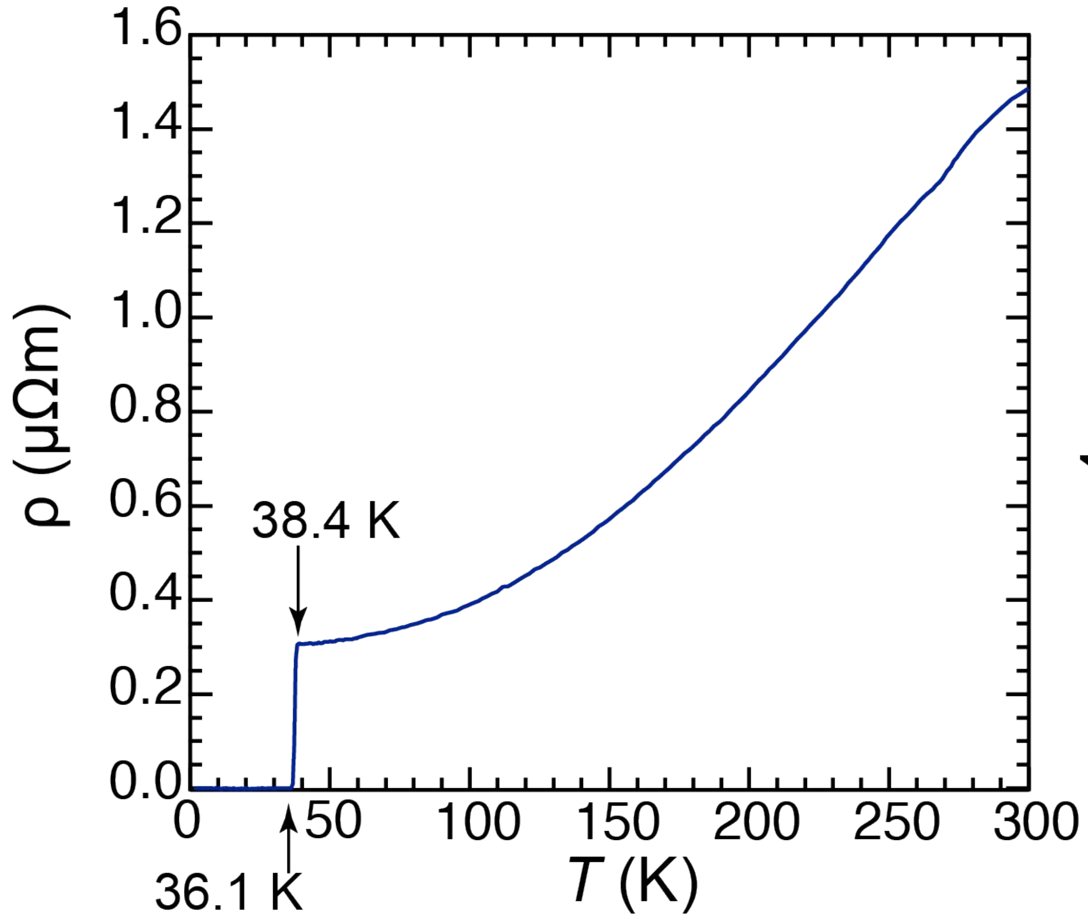

M-T

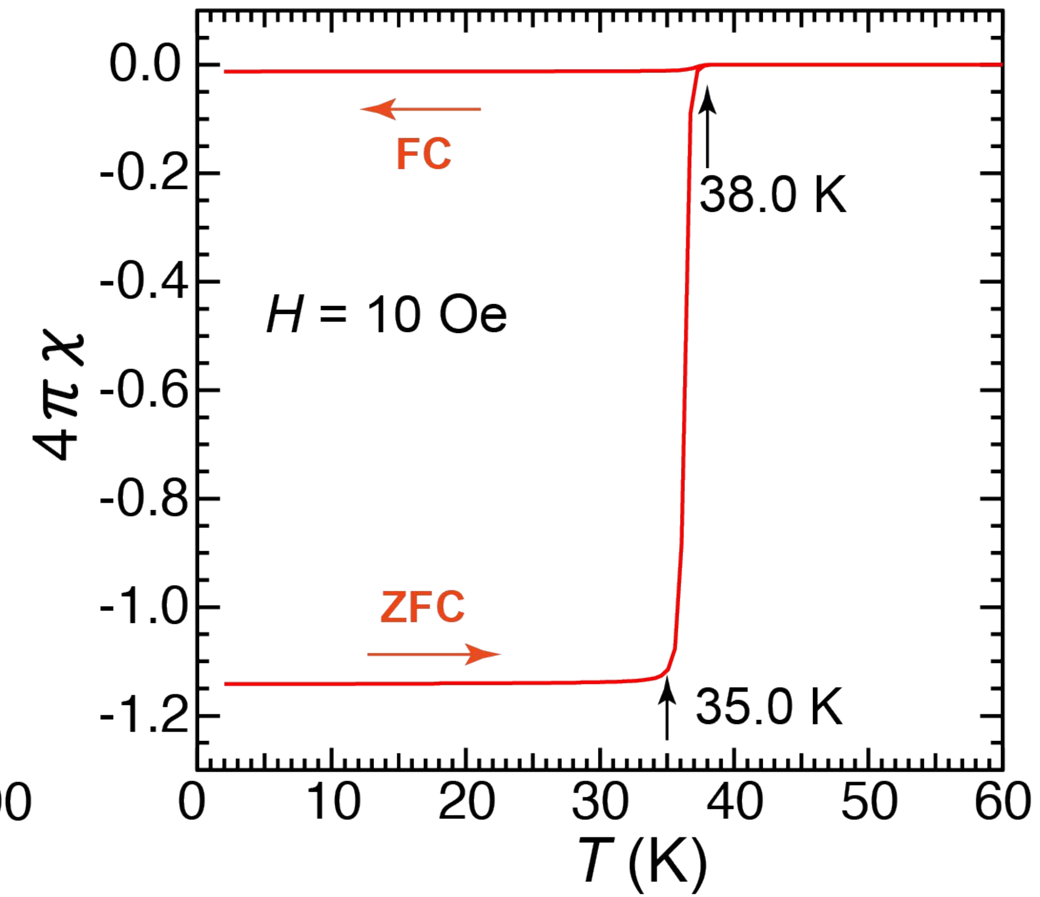

Superconducting properties

MgB /C system

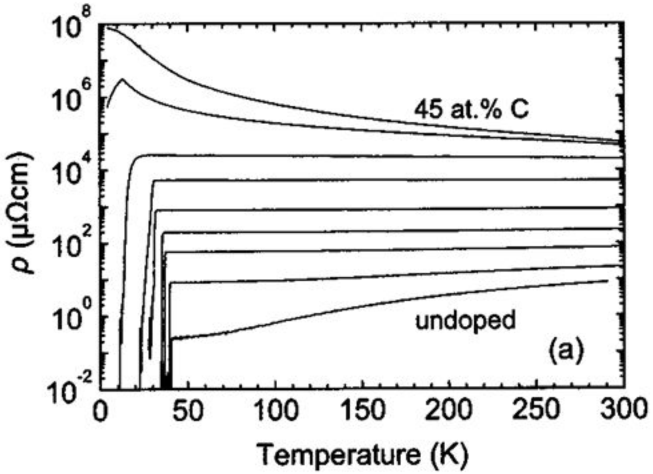

y ρ and magnetic susceptibility χ measurements

A. V. Pogrebnyakov et al. Appl. Phys. Lett. 85, 2017 (2014).

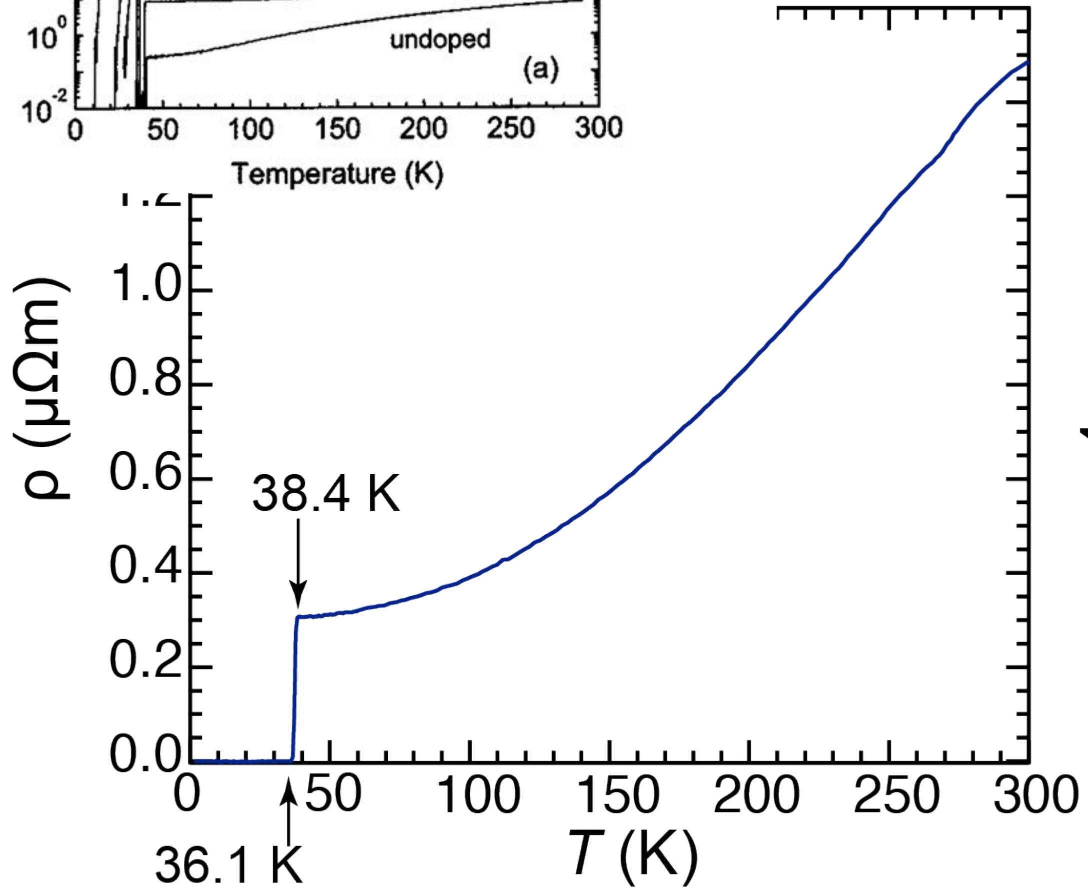

M-T

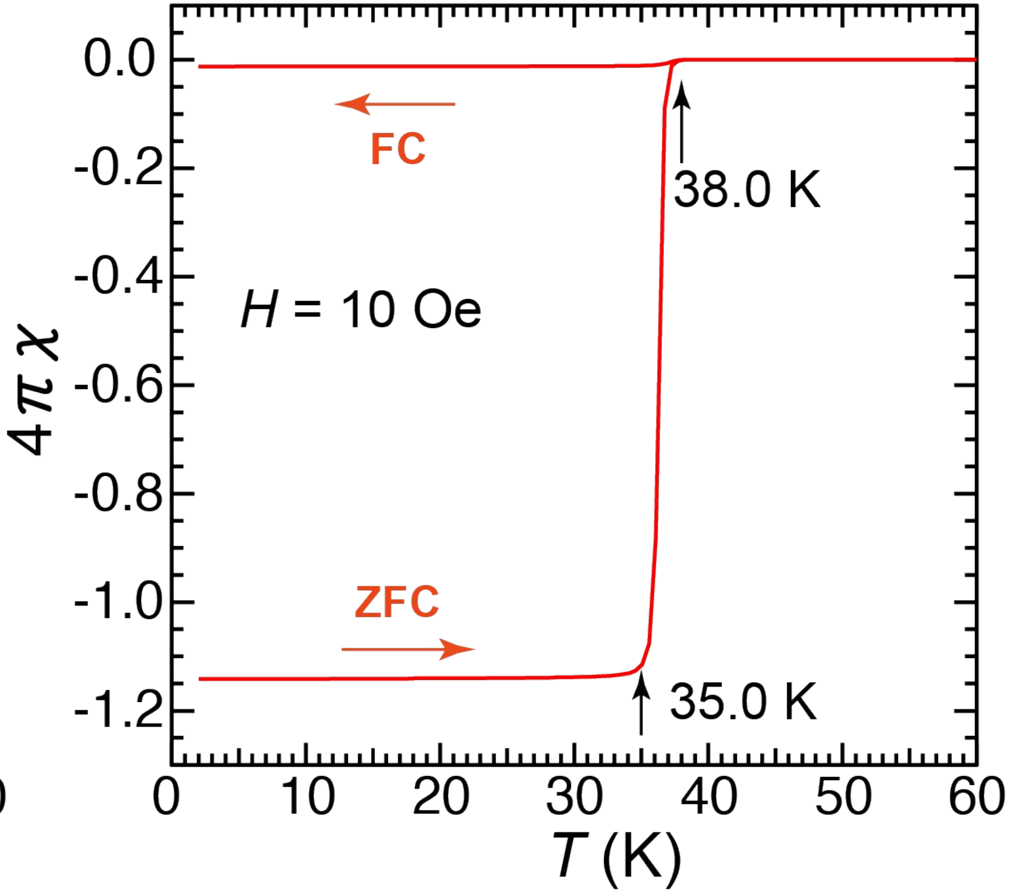

Superconducting properties

Electrical resistivity ρ and magnetic susceptibility χ measurements

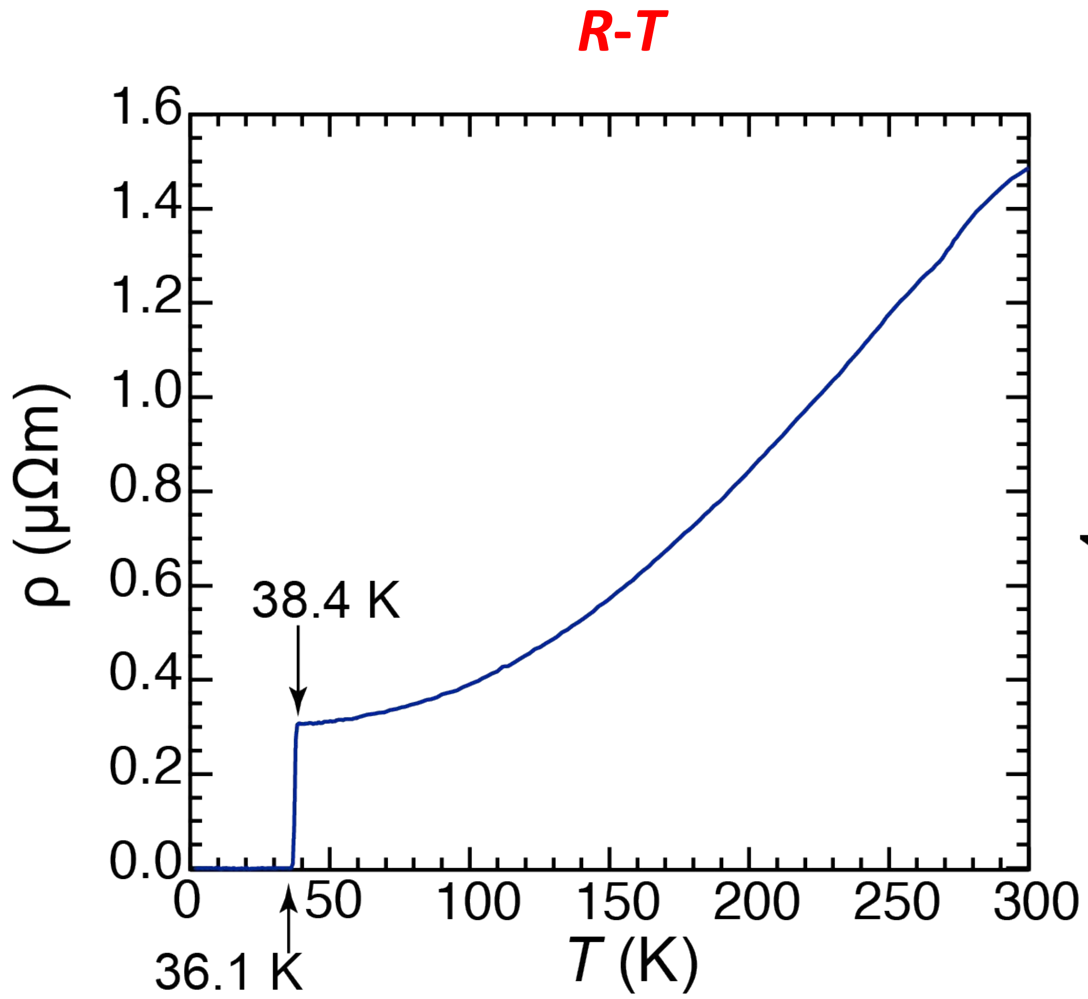

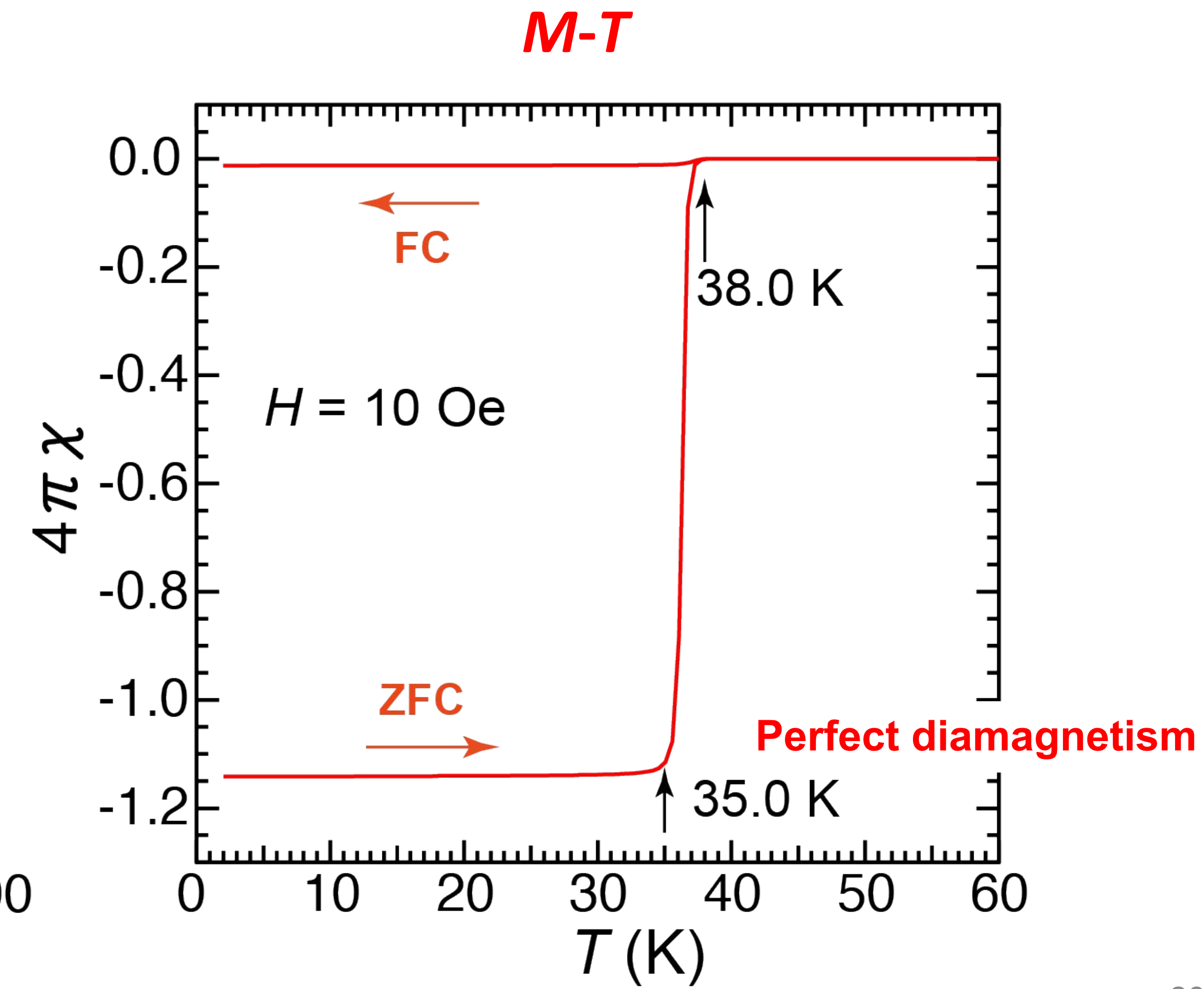

A global Josephson phase coherence is achieved, showing a bulk-like superconducting behavior.

Superconducting properties

Magnetoresistivity measurements

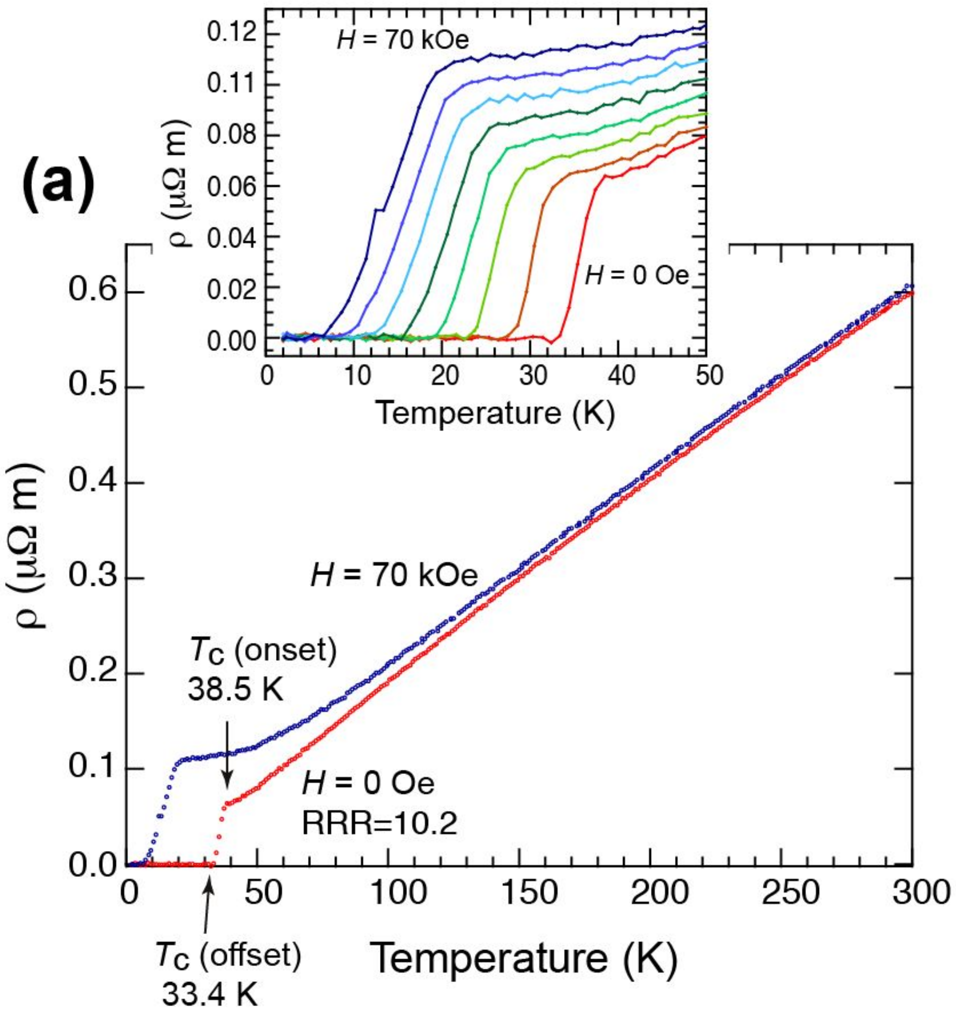

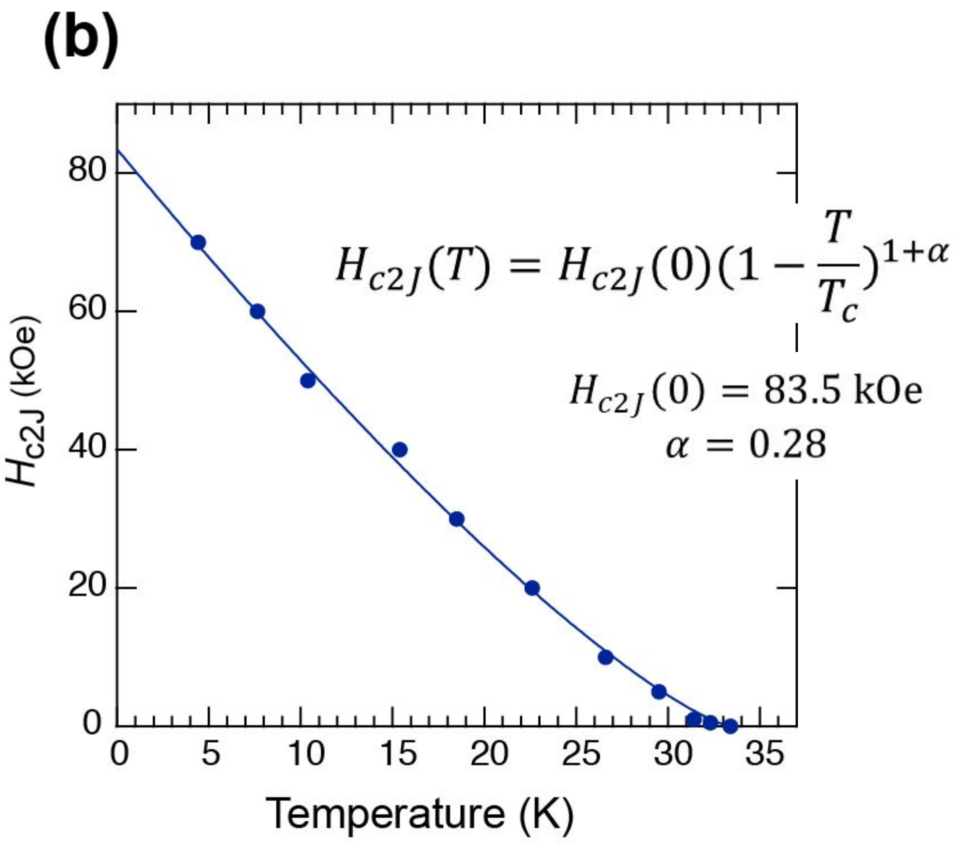

Estimation of Josephson coherence length and penetration depth

Ginzburg-Landau theory

$$H_{c2} = \Phi_0/(2\pi\xi^2) \qquad H_{c1} = \frac{\Phi_0}{4\pi\lambda^2}\ln(\frac{\lambda}{\xi})$$

$$H_{c1J} = 96\ \mathrm{Oe}\ , H_{c2J} = 83.5\ \mathrm{kOe}$$

$$\xi_J = 6\ \mathrm{nm}$$

$$\lambda_J = 252\ \mathrm{nm}$$

Ginzburg-Landau parameter $\kappa = \frac{\lambda_J}{\xi_J} = \sim 42 \gg 1$

Type II superconductor

走査 SQUID 顕微鏡(SSM)による超伝導渦糸の観察

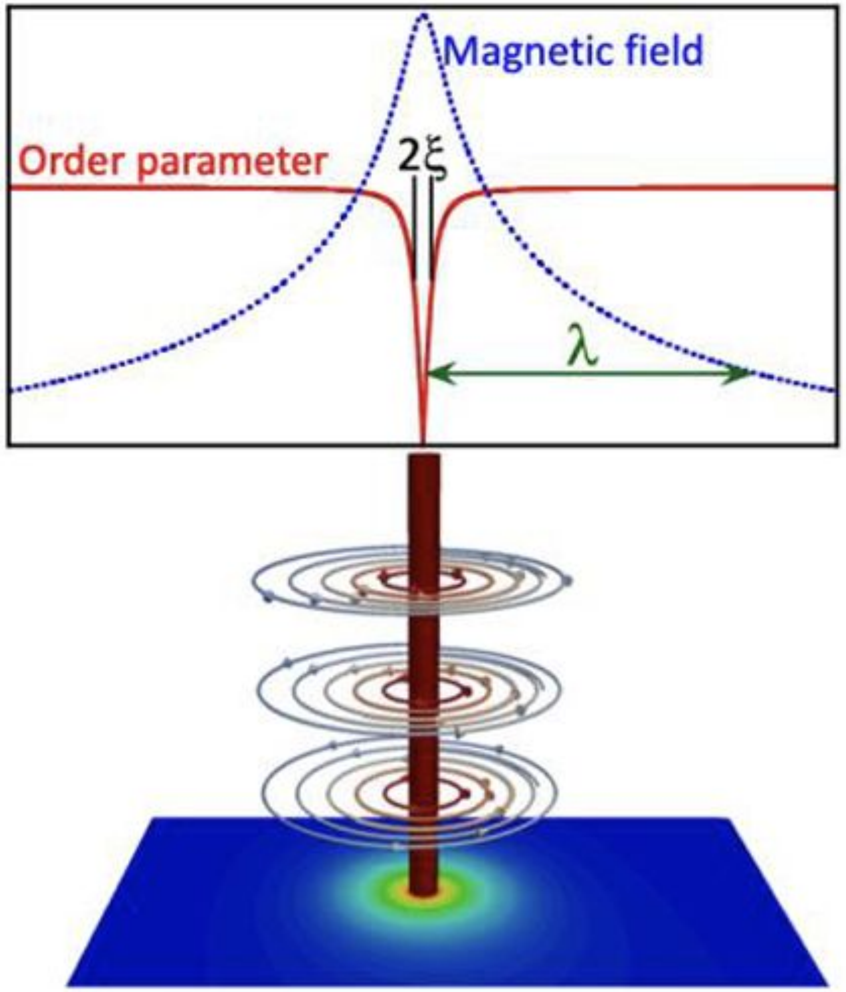

Schematic illustration of SC vortex

A. Glatz *et al.* J. Supercon. Novel Mag. 33, 127–141 (2020).

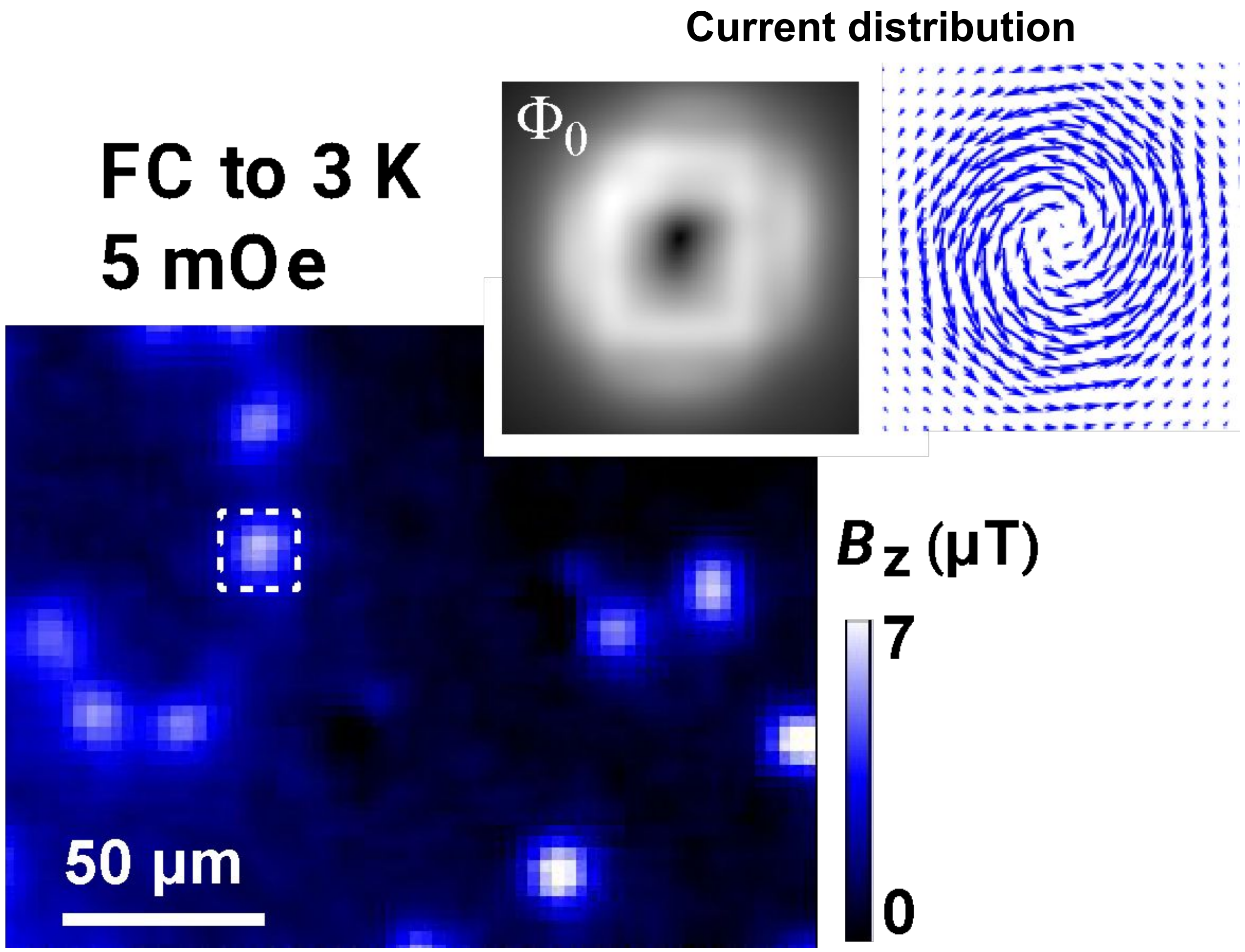

Scanning SQUID microscope image

磁気光学顕微鏡による磁束観察

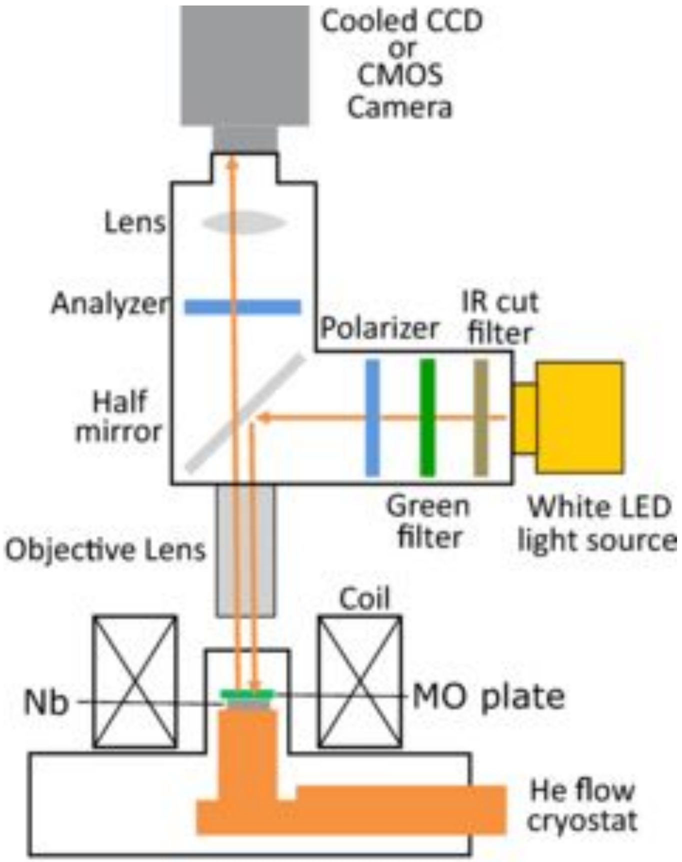

S. Ooi *et al.*, *Phys. Rev. B*, **104**, 064504 (2021).

Schematic of a MO microscope based on the Faraday effect in a sensor film placed on the surface of a magnetic sample.

磁気光学顕微鏡による磁束観察

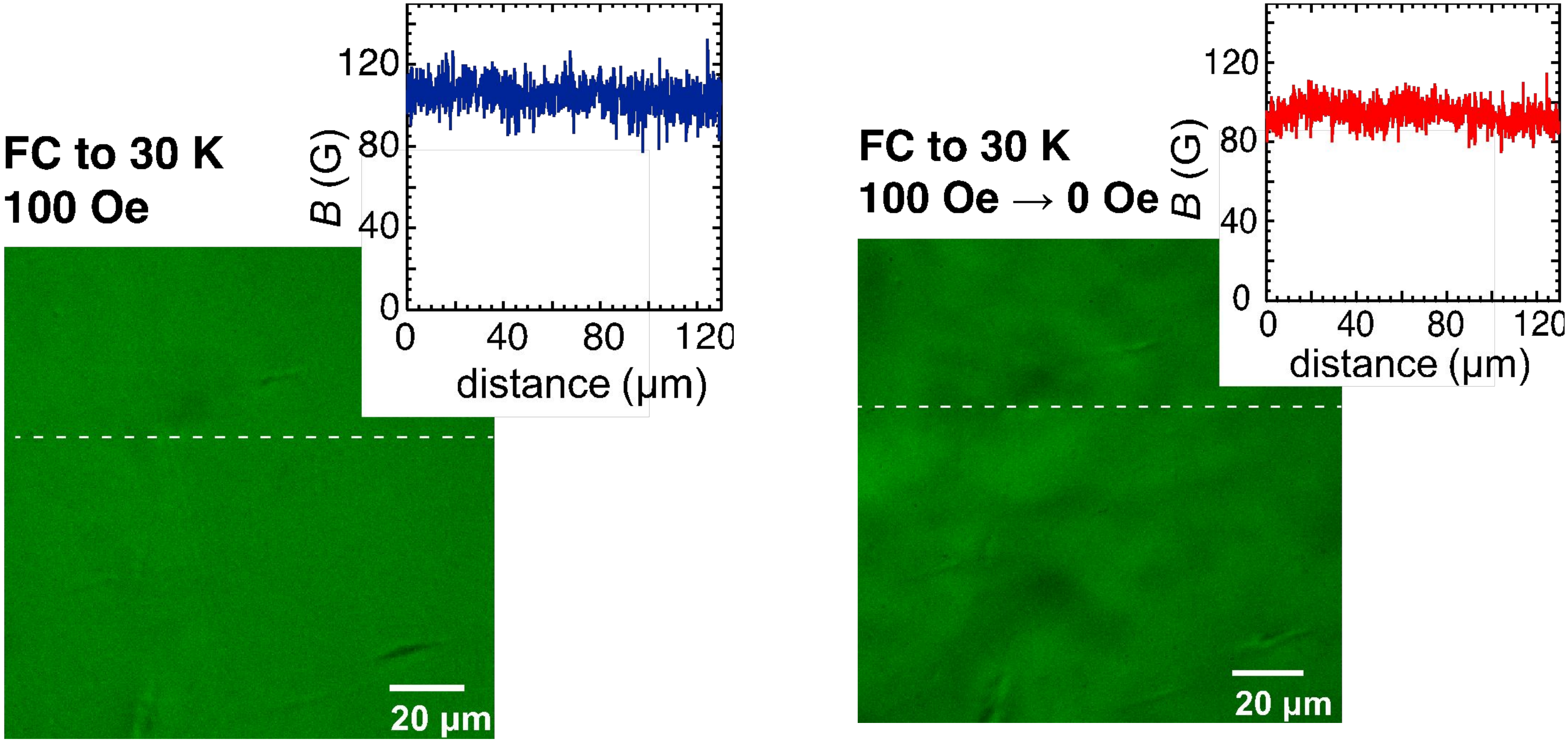

残留磁化状態：超伝導領域にピン留めされた磁束
試料全体に分布

残留磁化状態における渦糸電流分布

絶対強度

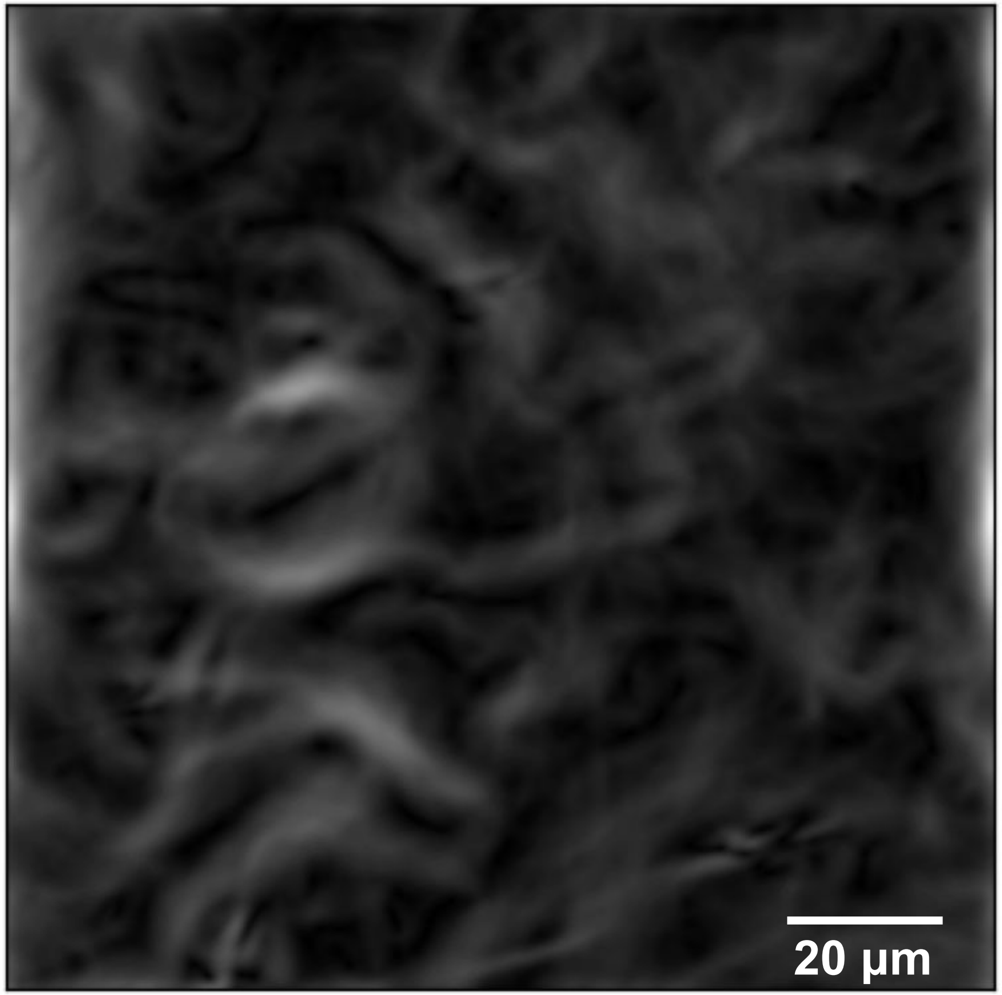

ベクトル図

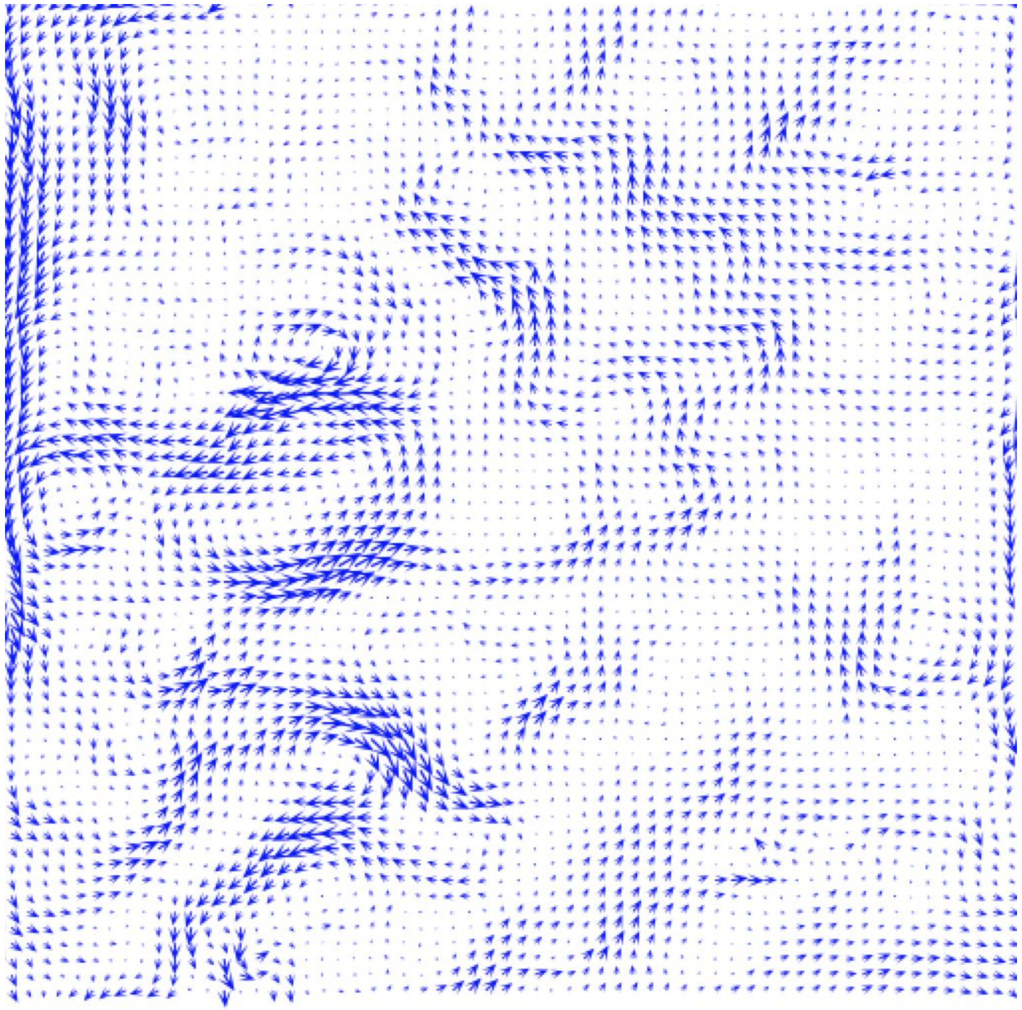

試料全体にわたって渦糸電流が分布：常伝導領域にランダムにピン留めされた超伝導渦糸の存在
粒界も高い臨界電流密度を保持

臨界電流密度J_cとピンニング力解析

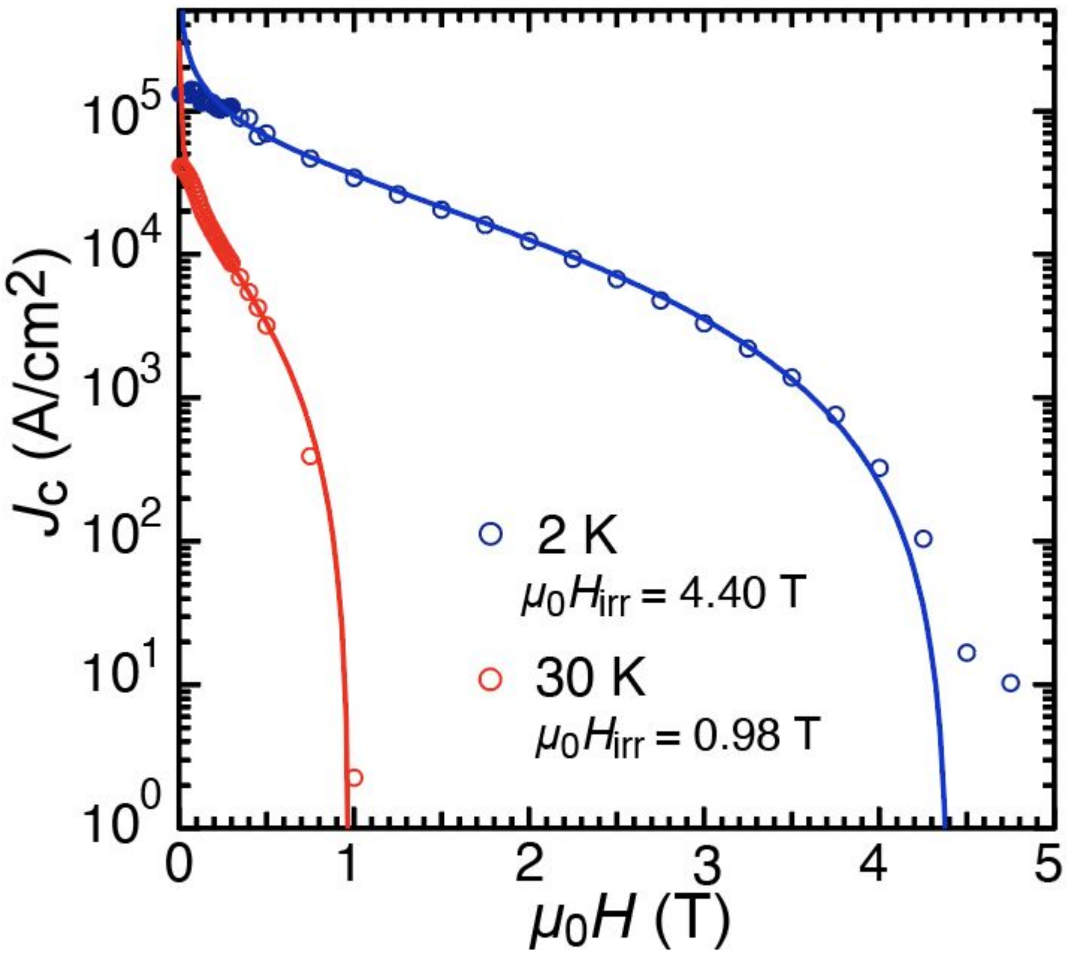

$$J_c = \frac{[1 - H/H_{irr}]^2}{\sqrt{H/H_{irr}}}$$

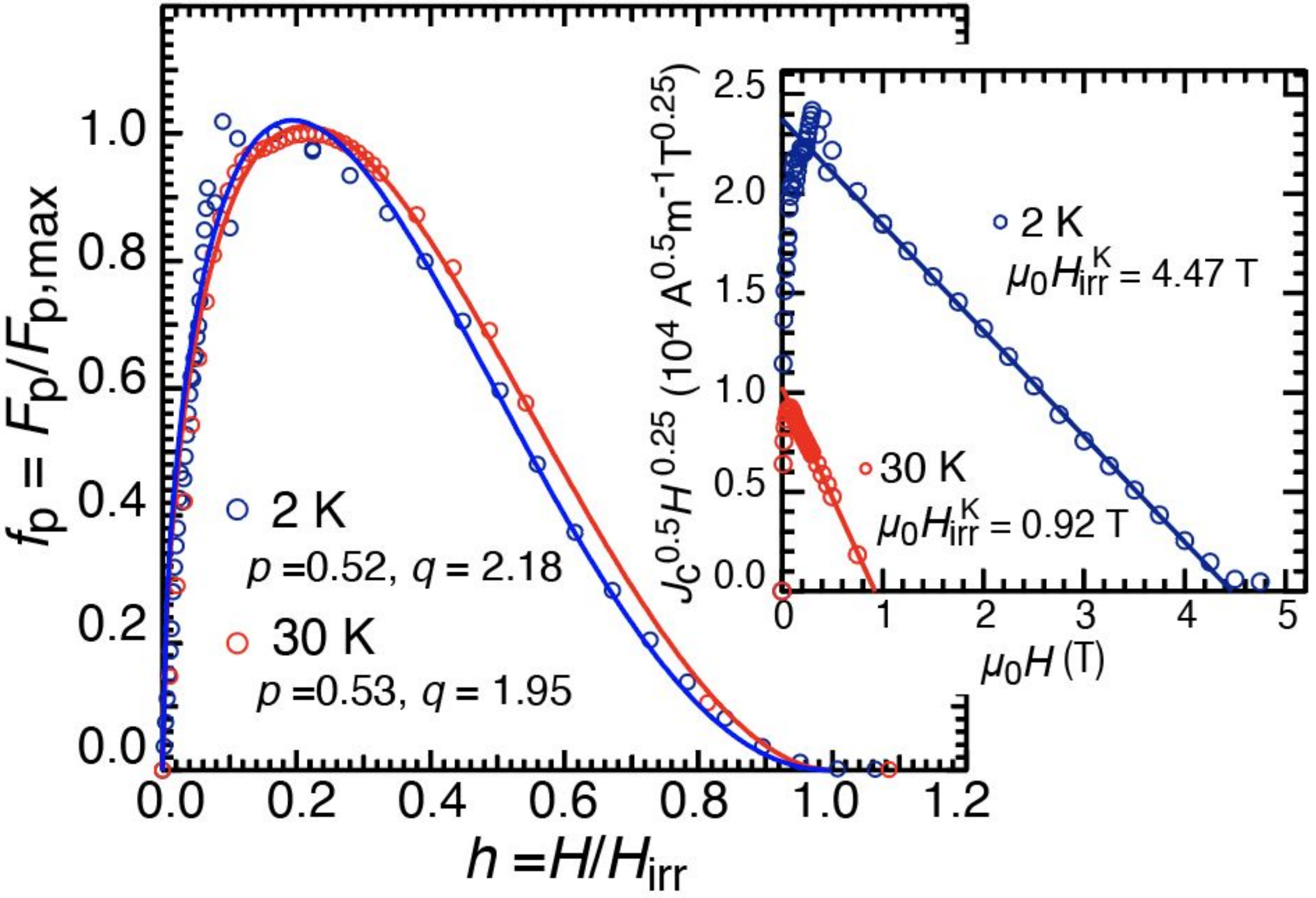

$$f_p \propto h^p (1-h)^q$$

スケーリング則の成立：等方的界面ピンニング機構

FESEM/EDX, TEM/EDX and HR-TEM measurements

B: red
Mg: blue
O: green

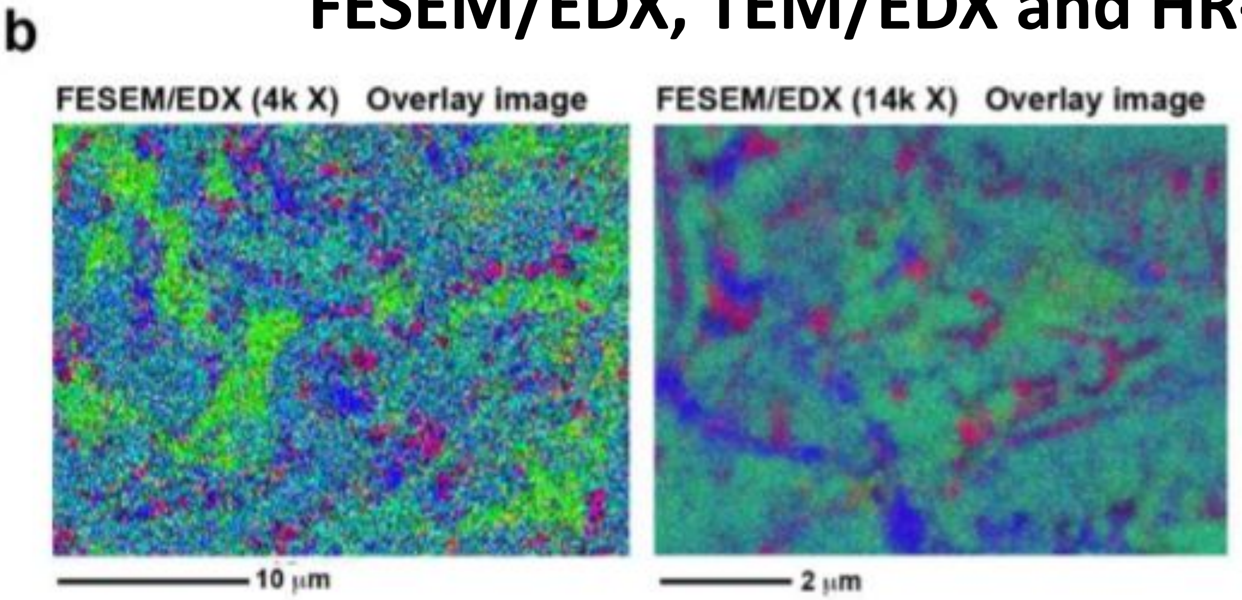

Low (x4,000) Magnification

Medium (x14,000) Magnification

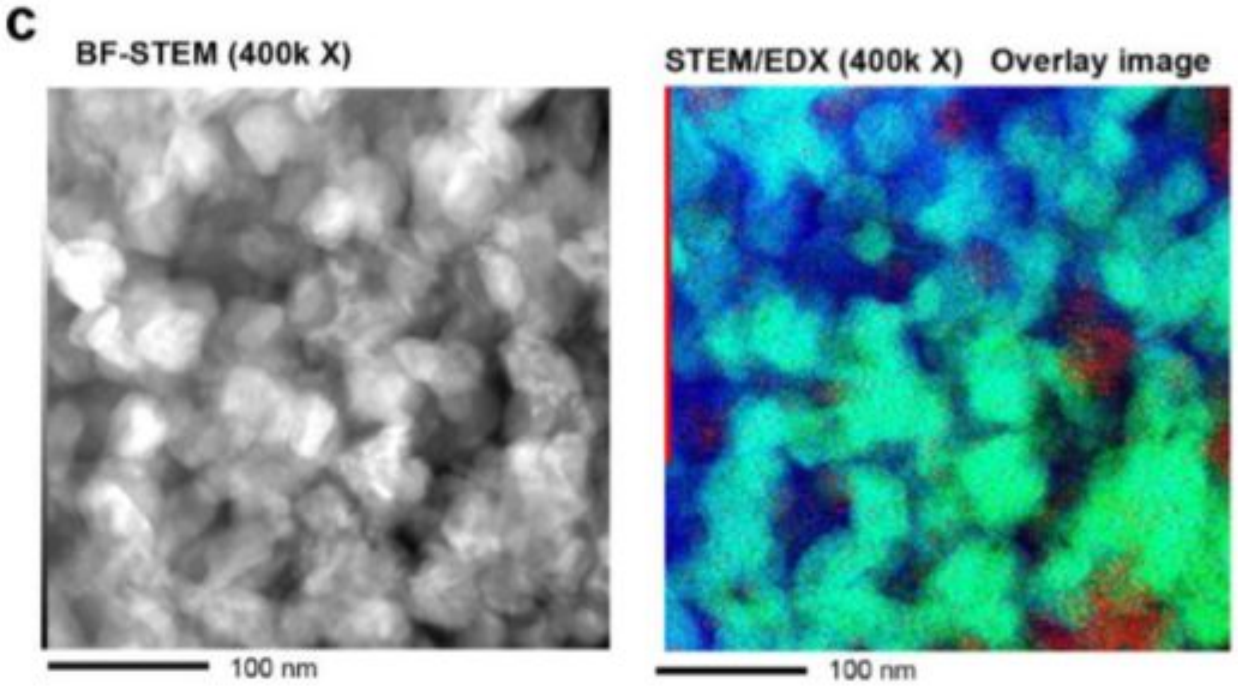

HR-TEM High (x4,000,000) Magnification

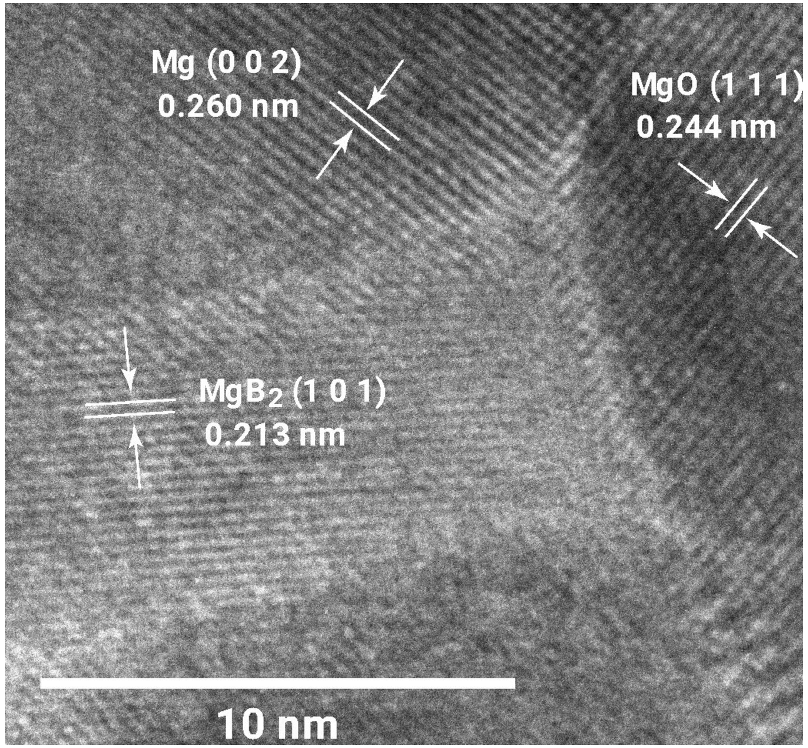

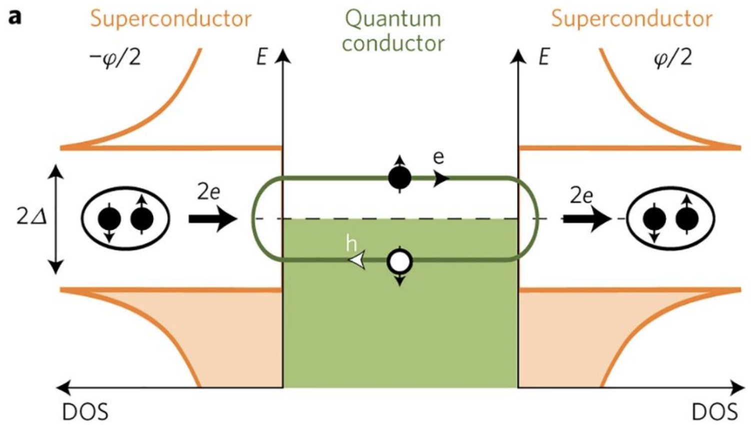

Proposed mechanism of the formation of the bulk like superconductivity

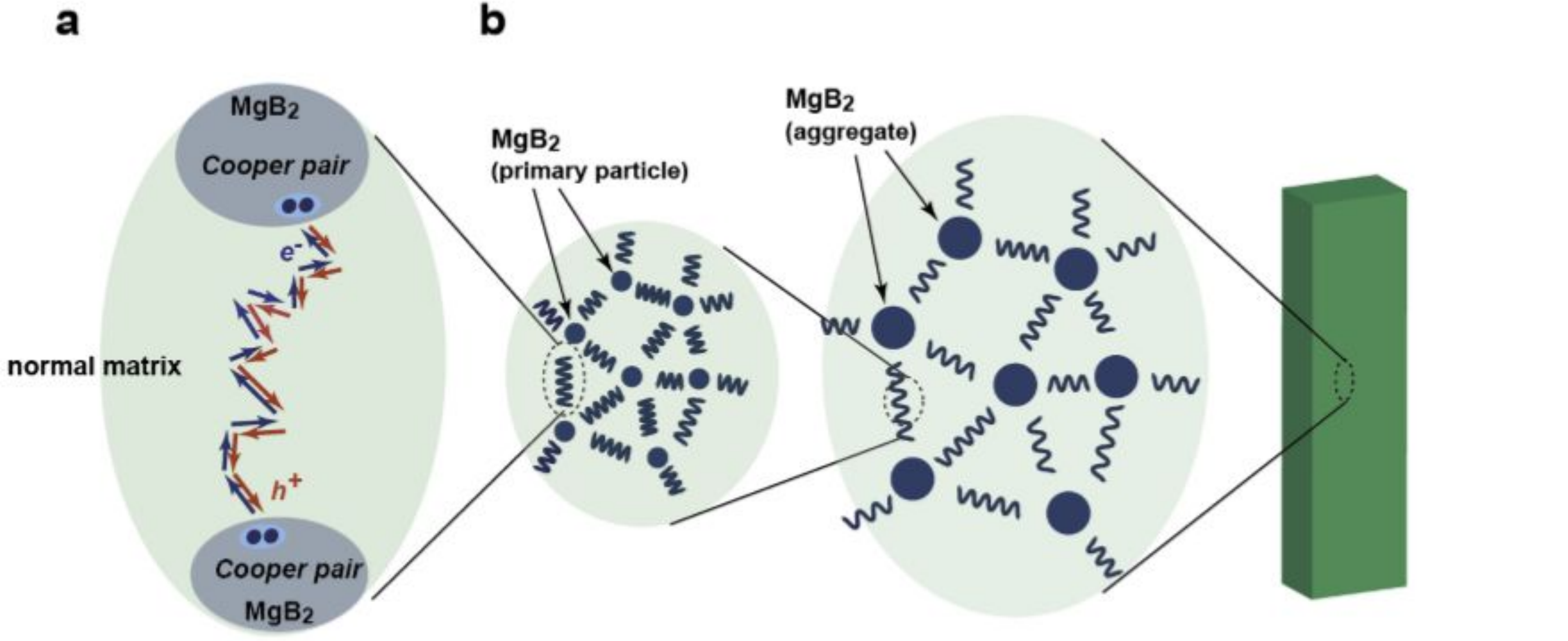

Phase-coherent Andreev reflection in the diffusive normal matrix

Long-range proximity coupling in the scale-free Josephson junction network

Global superconducting state

フラクタルネットワークを介した超伝導近接効果の階層的発現

強固な三次元的位相整合状態の形成

Future works

Synthesis and investigation of proximitized materials using nanocomposites.

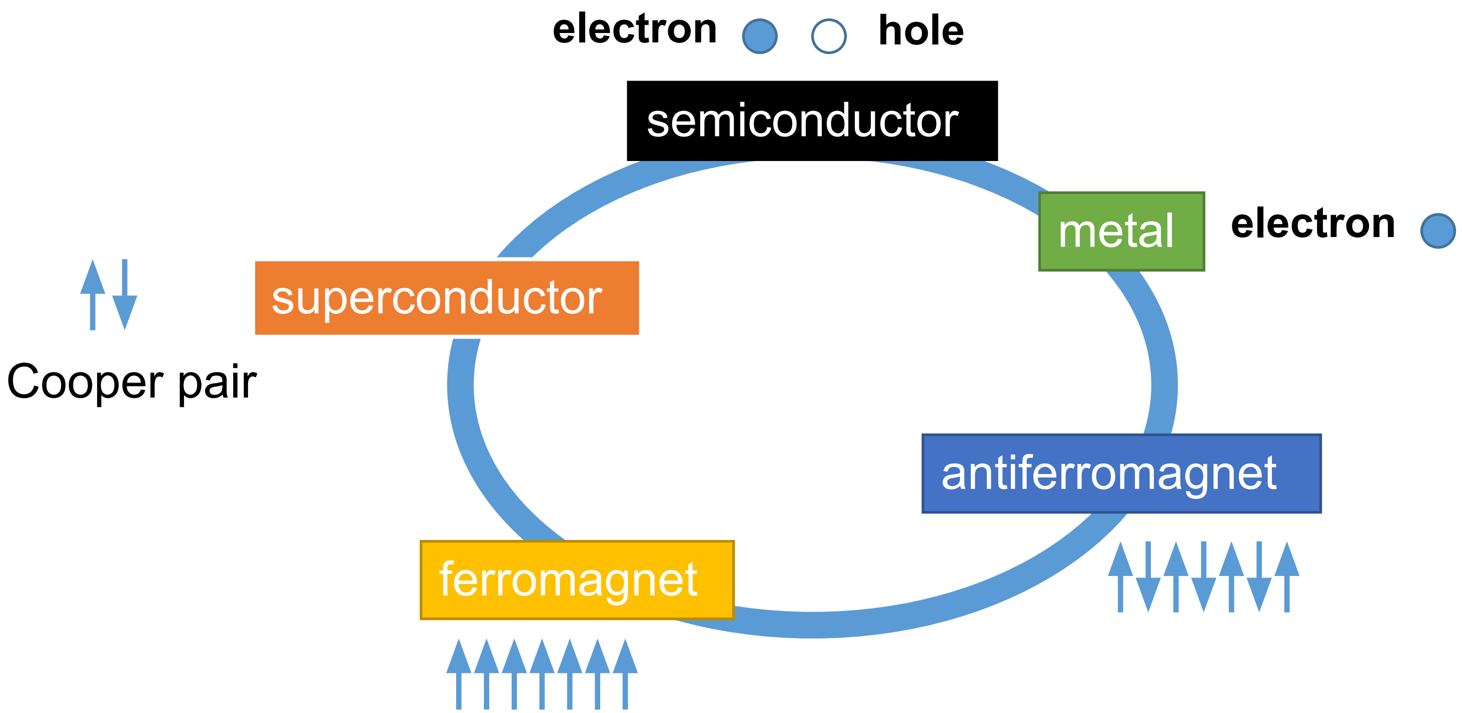

ありがとうございました